"Interaction and electron transfer between ferredoxin-NADP^{+} oxidoreductase and its partners: structural, functional and physiological implications"

[1]Paula Mulo and [2]Milagros Medina*

[1] Molecular Plant Biology, University of Turku, 20520 Turku, Finland

[2] Departamento de Bioquímica y Biología Molecular y Celular, Facultad de Ciencias, and Institute of Biocomputation and Physics of Complex Systems, Universidad de Zaragoza, 50009, Zaragoza, Spain

[‡]Correspondence to: Milagros Medina, Departamento de Bioquímica y Biología Molecular y Celular. Facultad de Ciencias, Universidad de Zaragoza. Pedro Cerbuna, 12. 50009 Zaragoza, Spain. Tel: +34976762476; Fax: +34976762123. E-mail: mmedina@unizar.es

1

(For nomenclature and classification of FNR isoforms in different higher plant species, please see Mulo 2011)

Summary

Ferredoxin–NADP$^+$ reductase (FNR) catalyzes the last step of linear electron transfer in photosynthetic light reactions. The FAD cofactor of FNR accepts two electrons from two independent reduced ferredoxin molecules (Fd) in two sequential steps, first producing neutral semiquinone and then the fully anionic reduced, hydroquinone, form of the enzyme (FNR$_{hq}$). FNR$_{hq}$ transfers then both electrons in a single hydride transfer step to NADP$^+$. We are presenting the recent progress in studies focusing on Fd:FNR interaction and subsequent electron transfer processes as well as on interaction of FNR with NADP$^+$/H followed by hydride transfer, both from the structural and functional point of views. We also present the current knowledge about the physiological role(s) of various FNR isoforms present in the chloroplasts of higher plants and the functional impact of subchloroplastic location of FNR. Moreover, open questions and current challenges about the structure, function and physiology of FNR are discussed.

Keywords: ferredoxin; ferredoxin-NADP$^+$ reductase; electron transfer; hydride transfer; photosynthesis; chloroplast

(For nomenclature and classification of FNR isoforms in different higher plant species, please see Mulo 2011)

1.-Photosynthetic Ferredoxin-NADP$^+$ reductase: general features and structure

The primary function of photosystem I (PSI) at the end of the linear photosynthetic electron transfer (PET) chain is to reduce NADP$^+$ to NADPH, mainly used as reducing power in the assimilation of CO_2 (Vishniac and Ochoa 1952). In plants and cyanobacteria this occurs via reduction of the soluble plant-type [2Fe–2S] ferredoxin (Fd) by PSI (Setif 2006), with the subsequent reduction of NADP$^+$ being catalyzed by the flavoenzyme ferredoxin–NADP$^+$ reductase (FNR, EC 1.18.1.2), according to the reaction 2Fd$_{rd}$ + NADP$^+$ $\rightarrow$2Fd$_{ox}$ + NADPH (Arnon 1991, Arnon and Chain 1975). In this process the FAD cofactor of FNR accepts two electrons in two sequential steps from two independent Fd$_{rd}$ molecules, first producing the neutral semiquinone and then the fully anionic reduced or hydroquinone form of the enzyme (FNR$_{hq}$). FNR$_{hq}$ transfers then both electrons in a single hydride transfer (HT) step to NADP$^+$ (Batie and Kamin 1984b, Carrillo and Ceccarelli 2003, Medina and Gómez-Moreno 2004). The reaction is a reversible process proposed to work in an ordered two-substrate process within a ternary Fd:FNR:NADP$^+$ complex, with the pyridine nucleotide binding first to FNR (Batie and Kamin 1984a, Batie and Kamin 1984b).

The relationships of plastidic FNRs ($\sim$35-36 kDa) with other enzymes showing FNR activity indicated that they share evolutionary origin with bacterial FNRs (also known as FPRs) (Aliverti, et al. 2008, Arakaki, et al. 1997, Ceccarelli, et al. 2004). Plastidic and bacterial FNRs all together form the plant-type FNR family, whose two-domain structure provides the basic scaffold for an extended superfamily of electron transfer (ET) flavoproteins (Fig. 1A) (Deng, et al. 1999, Dorowski, et al. 2001, Karplus, et al. 1991, Kurisu, et al. 2001, Muraki, et al. 2010, Serre, et al. 1996). The N-terminal FAD-binding domain is made up of six antiparallel β strands organized in two perpendicular β sheets, with a short α helix at the bottom and another α helix and a long loop that is maintained by a small two-stranded antiparallel β sheet at the top, while the C-terminal NADP$^+$-binding domain consists of a core of five parallel β strands surrounded by seven α helices (Fig. 1A). The FAD is bound outside the antiparallel β barrel, and its isoalloxazine ring lies between two tyrosines, one belonging to the FAD binding domain (Y79 in *Anabaena* FNR, *An*FNR) and the other to the NADP$^+$-binding domain (the C-terminal Tyr, Y303 in *An*FNR) (Fig. 1B). Although the main physiological

(For nomenclature and classification of FNR isoforms in different higher plant species, please see Mulo 2011)

function of plastidic FNRs is the production of reducing power in the form of NADPH, these enzymes are reversible and also catalyze the reduction of Fd_{ox} by NADPH to provide reducing power to various metabolic processes (Hanke and Mulo 2013). This is possible because the midpoint reduction potentials of the molecules involved in the reaction are in the same range. The two one-electron midpoint potentials of the FAD cofactors in plastidic FNRs are close to each other, and therefore they stabilize only 10–20% of the maximal amount of semiquinone, with $E_{ox/hq}$ values ranging among -325 mV and -370 mV when considering different species (Batie and Kamin 1986, Cassan, et al. 2005, Corrado, et al. 1996, Faro, et al. 2002b, Sánchez-Azqueta, et al. 2012). $E_{ox/hq}$ for Fd is $\sim$–420 mV and that of $NADP^+$ –320 mV (Pueyo and Gómez-Moreno 1991). Differences in redox potentials explain that the reaction goes more easily towards the production of NADPH, required in high yields in photosynthetic carbon assimilation, than into the opposite direction for the production of compounds required in lower amounts in dark metabolism. In addition, interaction makes PET thermodynamically more favorable. Fd:FNR complex formation makes the Fd midpoint potential more negative (~15 mV in *An*Fd) and that of FNR less negative (27–40 mV in *An*FNR). In addition, formation of the FNR:$NADP^+$ complex makes de the midpoint reduction potential for reduction of $NADP^+$ less negative as compared to the free coenzyme form (Batie and Kamin 1984a, Batie and Kamin 1986, Hurley, et al. 1997).

Higher plants contain a small gene family encoding at least two distinct chloroplast-targeted FNR isoforms (Green, et al. 1991, Grzyb, et al. 2008, Hanke, et al. 2005, Morigasaki, et al. 1993). Despite high sequence identity between the FNR isoforms, in all higher plant species studied to date one of them appears to be basic (pI above 6) and the other one acidic (pI around 5) (Hanke, et al. 2005). The single *fnr* knock-out mutants are viable indicating redundancy of function, whereas double mutants are lethal (Hanke, et al. 2008, Lintala, et al. 2009, Lintala, et al. 2007, Lintala, et al. 2012). In cyanobacteria, the two forms of FNR, differing in size (FNR(S) and FNR(L)), originate from a single gene (Thomas, et al. 2006). The longer form FNR(L), which is bound to the phycobilisome antenna, has been indicated in the photoreduction of $NADP^+$, whereas the small, soluble FNR(S) has been suggested to function in opposite direction (Thomas, et al. 2006). In addition to the well

(For nomenclature and classification of FNR isoforms in different higher plant species, please see Mulo 2011)

characterized photosynthetic role of FNR in the last step of linear PET, it has been suggested to participate in cyclic electron transfer (CET) around PSI (DalCorso, et al. 2008, Iwai, et al. 2010, Joliot and Joliot 2002, Laisk, et al. 2007, Shahak, et al. 1981). In CET, lumenal ΔpH accumulates without production of reducing equivalents (i.e. NADPH), which enables to fulfil the high demand of ATP in C4 plants (Rumeau, et al. 2007). In C3 plants CET has been suggested to play a crucial role upon acclimation to adverse environmental conditions, yet the exact functional details and components are not known (Suorsa 2015). Accordingly, also the role of FNR in CET has remained elusive (Goss and Hanke 2014). Similarly to cyanobacteria, in higher plants FNR is distributed between the membrane-bound and the soluble pool (Forti and Bracale 1984, Fredricks and Gehl 1982, Matthijs, et al. 1986). Recently, novel mechanisms and components of FNR membrane tethering have been revealed (see below; (Benz, et al. 2009, Jurić, et al. 2009, Yang, et al. 2016), but the ultimate physiological significance of FNR allocation on energy distribution still requires further studies.

2.-Molecular interactions and electron transfer processes between FNR and its photosynthetic redox partners: Fd and NADP$^+$

PET from Fd to NADP$^+$ requires the formation of at least two binary transient complexes: Fd:FNR and FNR:NADP$^+$. These complexes arrange their respective [2Fe-2S], isoalloxazine and nicotinamide redox centers, when present in the adequate redox states, at the proper distance and orientation for the high efficiency exhibited in the overall PET process. Extensive kinetics, chemical modification, mutational, thermodynamic, binding and structural determinations were reported in the last 50 years to characterize the interaction surfaces in the Fd:FNR and FNR:NADP$^+$ complexes. These studies identified key residues for the interaction, binding induced conformational changes and ET processes, reviewed in the previous decade (Carrillo and Ceccarelli 2003, Hurley, et al. 2002, Medina 2009, Medina and Gómez-Moreno 2004). Recent breakthroughs in computational structural biology have also provided interesting clues to the overall dynamics of interaction and ET processes within the Fd:FNR and FNR:NADP$^+$ complexes at the molecular and atomic levels. Indeed, integration of experimental data accumulated during the years with results from

(For nomenclature and classification of FNR isoforms in different higher plant species, please see Mulo 2011)

theoretical methods has proved to be essential for the better understanding of these processes.

2.1. Fd:FNR interaction and subsequent ET processes.

Early studies already pointed to the role of electrostatic forces in facilitating productive Fd:FNR interactions (Batie and Kamin 1984a, Batie and Kamin 1984b, Bhattacharyya, et al. 1987, Foust, et al. 1969, Jelesarov, et al. 1993, Medina, et al. 1992a, Medina, et al. 1992b, Medina, et al. 1992c, Walker, et al. 1990, Zanetti, et al. 1984, Zanetti, et al. 1979), and soon it was also accepted that hydrophobic effects would play a key role in complex stability (Jelesarov and Bosshard 1994). Site-directed mutagenesis, steady-state and transient kinetic measurements, together with structural determinations and calorimetric studies, were then used in an attempt to describe this system at the molecular level (Aliverti, et al. 1991, Aliverti, et al. 1993, Hurley, et al. 1993a, Hurley, et al. 1993b). Combination of these methodologies identified key residues at the interaction surfaces of these proteins as well as in the modulation of their redox centers, ascribing major and specific functions to some of them as reviewed elsewhere (Hurley, et al. 1999, Hurley, et al. 1994, Hurley, et al. 2002, Medina and Gómez-Moreno 2004) (Fig. 1C-E). Moreover, FNR active site residues, namely S80, E301 and the C-terminal Y303, as well as some residues at the FAD-binding domain, namely R16, L76, L78 and particularly K75 (*Anabaena* numbering, Figures 1A-C) are crucial in modulating the midpoint reduction potential and stabilizing the semiquinone, a key factor for efficient one-ET processes between Fd and FNR (Aliverti, et al. 1995, Aliverti, et al. 1998, Faro, et al. 2002a, Martínez-Júlvez, et al. 1998a, Martínez-Júlvez, et al. 2001, Medina, et al. 1998, Nogués, et al. 2004). These studies indicated that charged residues on the surfaces of Fd and FNR provided with a dipole moment that helped their mutual relative orientation and made possible their first encounter (Fig. 1). In addition, it was shown that the mutual disposition between Fd and FNR after the first encounter is not optimal, but a reorientation situating the [2Fe-2S] and isoalloxazine redox centers at the right distance and orientation is required for efficient electron exchange. Short range electrostatic interactions (particularly salt-bridges) were then shown to contribute to such reorganization, in general Fd providing negative charged residues and FNR positive ones (Fig. 1C and 1F)

6

(For nomenclature and classification of FNR isoforms in different higher plant species, please see Mulo 2011)

(Aliverti, et al. 1994, Hurley, et al. 1999, Hurley, et al. 1996, Martínez-Júlvez, et al. 1998a, Martínez-Júlvez, et al. 1998b, Mayoral, et al. 2005, Medina and Gomez-Moreno 2004, Medina and Gómez-Moreno 2004). Moreover, coupling hydrophobic patches of residues and the release of water molecules at the protein-protein interface upon complexation were described as key elements to provide the reorganization energy favoring the orientation in which the ET occurs efficiently (Hurley, et al. 1993a, Hurley, et al. 2002, Jelesarov and Bosshard 1994, Kinoshita, et al. 2015, Martínez-Júlvez, et al. 2001, Medina and Gómez-Moreno 2004). The FNR two-domain arrangement was also shown to play an important role in the overall process (Fig. 1A and 1C). The open inter-domain cavity at the interface and the loops at its edge (particularly the loop allocating the FAD adenosine, loop 102-114 in *An*FNR) provide additional flexibility to accommodate the protein partner during the catalysis (Sánchez-Azqueta, et al. 2014c). Finally, some negative residues on the FNR surface introduce repulsive interactions for Fd approaching the NADP$^+$-binding domain (as E139 in *An*FNR), also contributing to improve the optimal orientation for the ET (Faro, et al. 2002a, Hurley, et al. 2000).

As expected for a transient interaction, dissociation constants for the Fd:FNR complex are in the low micromolar range for all the evaluated species (4-10 µM) (Aliverti, et al. 1994, Hurley, et al. 2002, Martínez-Júlvez, et al. 2009, Medina and Gómez-Moreno 2004, Medina, et al. 1998, Nogués, et al. 2004, Velázquez-Campoy, et al. 2006). Formation of the complex is both enthalpically and ectopically driven at pH 8, with a release of water molecules and protonation of at least one ionizable group (proposed as at least E82 in *Spinacea oleracea* Fd, *Sp*Fd, and H299 in *An*FNR) (Jelesarov and Bosshard 1994, Martínez-Júlvez, et al. 2009, Piubelli, et al. 1997). Nevertheless, intrinsic binding parameters obtained at high pH values where no protonation occurs indicated that complex formation is entropically driven with negligible enthalpic contribution.

Crystallographic three dimensional structures corresponding to the *Anabaena* and maize binary Fd:FNR complexes were reported almost simultaneously (Kurisu, et al. 2001, Morales, et al. 2000). In these structures the redox centers of both proteins are in close proximity; the shortest distances being 7.4 and 6.0 Å, respectively, between the C8 of the flavin isoalloxazine and the [2Fe-2S] cluster (Fig. 2A and 2B). In

(For nomenclature and classification of FNR isoforms in different higher plant species, please see Mulo 2011)

agreement with biochemical and biophysical studies, these structures show a dipole moment complementarity as well as short range electrostatic intermolecular interactions occurring through salt bridges, with the interfaces near the prosthetic groups being hydrophobic (Fig. 1 and 2). Noticeably, structures of Fd and FNR in the complex and in the free state show some differences. In *Zea mays*, Fd binding to FNR (*Zm*FNR) induces the formation of a H-bond between E312 and S96 in the FNR active site, proposed to determine the optimal orientation of the two proteins for ET as well as to modulate the FNR enzymatic and redox properties (Aliverti, et al. 1998, Bruns and Karplus 1995, Kurisu, et al. 2001). In *Anabaena* FNR the same two residues (E301 and S80) are proposed to mediate proton transfer from the external medium to the FNR isoalloxazine N5 atom (Serre *et al.*, 1996). In this crystallographic association E301 is no more exposed to solvent but H-bonded to Fd S64, suggtesting a proton transfer pathway between the external medium and the FNR isoalloxazine in the complex (Faro, et al. 2002b, Mayoral, et al. 2000, Medina, et al. 1998). Moreover, conformational differences at the 46-47 peptide bond between the oxidized and reduced forms in *An*Fd were suggested to trigger complex dissociation as a function of the Fd redox state (Fig. 1C and 1D). Such changes might induce the transient displacement of the aromatic side chain of *An*Fd F65, a key residue for the interaction with hydrophobic patches on FNR (Hurley, et al. 1993a, Martínez-Júlvez, et al. 2001, Morales, et al. 1999, Morales, et al. 2000).

Therefore, a dynamic mechanism in which the initially formed Fd:FNR complex reorganizes prior to each ET and then disassembles upon a Fd redox-linked conformational change, is nowadays accepted. This mechanism balances a high turnover biological requirement with the need for specific binding, as also shown in other transient complexes (Schilder and Ubbink 2013, Ubbink 2012).

Although the formation of a transient complex between Fd and FNR during ET was extensively described using mutational, kinetic and crystallographic studies, recently computational tools have also added new aspects to our understanding of the mechanism. Rigid-body docking simulations with interface side-chain refinement (Medina, et al. 2008) as well as Brownian dynamics simulations (Khruschev, et al. 2015) explained the existence of alternative binding modes along the transient Fd:FNR

(For nomenclature and classification of FNR isoforms in different higher plant species, please see Mulo 2011)

interaction. These observations were in good agreement with crystallographic data and explained some previous experimental data by supporting formation of several transitory interactions during the overall process (Faro, et al. 2002a, Hurley, et al. 2002, Medina and Gómez-Moreno 2004). More recently, a multiscale modelling approach (including coarse-grained and all-atom protein-protein docking, the QM/MM e-Pathway analysis and electronic coupling calculations) has in addition provided a comprehensive electronic analysis of the ET process (Saen-Oon, et al. 2015). This study is consistent with ET within the Fd:FNR complex taking place in a dominant interprotein complex orientation through a bridge-mediated ET mechanism facilitated by Fd residues at the loop 40-49 (Fig. 2C). It also indicates a major role of the critical hydrophobic and salt-bridge interactions experimentally determined to discriminate the efficient ET configurations to the fraction placing the Fd loop at the interface and at short donor-acceptor distances between redox centers (Hurley, et al. 2002, Medina 2009, Medina and Gómez-Moreno 2004). Such conformations are similar to those identified by crystallography (Kurisu, et al. 2001, Morales, et al. 2000). It is worth to remember that the loop 40-49 in Fd contains the peptide bond (Fig. 1E) whose redox conformational differences are suggested to modulate complex association and dissociation (Morales, et al. 1999). Therefore, such a loop appears critical not only in the ET process itself but also in transient complex formation and dissociation.

2.2. FNR:NADP$^+$/H interaction and HT event.

The final photosynthetic reduction of NADP$^+$ by FNR$_{hq}$ occurs by a HT from the N5 of isoalloxazine anionic hydroquinone of the FAD cofactor to the N4 nicotinamide ring of the coenzyme (C4N). In photosynthetic enzymes this process is reversible and has been thoroughly analyzed from the mechanistic and structural points of view in higher plant and cyanobacterial enzymes (Arakaki, et al. 1997, Carrillo and Ceccarelli 2003, Tejero, et al. 2007). Two different transient charge-transfer complexes (CTC) form prior to and upon HT regardless of the HT direction, known as FNR$_{ox}$-NADPH (CTC-1) and FNR$_{hq}$-NADP$^+$ (CTC-2), producing an equilibrium mixture of CTCs (See Fig. 2-7 in (Tejero, et al. 2007) and Fig. 2 and 3 in (Sánchez-Azqueta, et al. 2012). Many of the factors and key residues which govern conformational changes in regions involved in coenzyme binding, as well as in determining coenzyme specificity for NADP$^+$ versus

(For nomenclature and classification of FNR isoforms in different higher plant species, please see Mulo 2011)

NAD$^+$ and reaction reversibility have been described in detail. Moreover, crucial residues in the isoalloxazine environment facilitate HT by modulating the isoalloxazine midpoint reduction potential and/or by contributing to the catalytically competent binding of the nicotinamide (Aliverti, et al. 2001, Arakaki, et al. 2001, Faro, et al. 2002b, Medina 2009, Medina, et al. 2001, Musumeci, et al. 2008, Peregrina, et al. 2009, Piubelli, et al. 2000, Sánchez-Azqueta, et al. 2014b, Sánchez-Azqueta, et al. 2014c, Sánchez-Azqueta, et al. 2012, Tejero, et al. 2003, Tejero, et al. 2005).

The different X-ray structures so far reported for the FNR:NADP$^+$ interaction in plant and cyanobacterial enzymes, using both wild-type (WT) and mutant proteins, further contributed to the mechanistic understanding of the process at the molecular level (Carrillo and Ceccarelli 2003, Deng, et al. 1999, Hermoso, et al. 2002, Serre, et al. 1996, Tejero, et al. 2005). Altogether experimental information indicated an enzyme:coenzyme interaction stepwise mechanism to approximate the C4N of the nicotinamide to the N5 of FAD to attaint efficient HT. NADP$^+$/H behaves as a bipartite ligand that binds to FNR with its two dinucleotide moieties in partially independent ways, with the complex being mainly stabilized by interactions involving the 2'P-AMP moiety of the dinucleotide (Batie and Kamin 1986). Three main FNR regions are responsible for the NADP$^+$/H coenzyme binding to attain the catalytically competent complex: the binding sites for the 2'-phospho-AMP (2'P-AMP), the pyrophosphate (PPi) and nicotinamide mononucleoside (NMN) moieties of NADP$^+$ (Deng, et al. 1999, Hermoso, et al. 2002, Tejero, et al. 2005). Recognition of the 2'P-AMP moiety of the coenzyme is presented as the first interaction stage, with Ser, Arg or Lys, and Tyr residues at the 2'P-AMP binding cavity determining coenzyme specificity and orientation (C-I in Fig. 3A and 3B) (Aliverti, et al. 1991, Medina, et al. 2001, Tejero, et al. 2007) (See Fig. 4 in (Tejero, et al. 2005)). The interaction of these residues with the 2'P-AMP portion induces conformational changes in both the protein and the coenzyme to perfectly fit the adenine and pyrophosphate moieties in their binding cavities (C-II in Fig. 3A and 3B). In such intermediate arrangement the 155–160 and 261–268 loops accommodate the coenzyme pyrophosphate portion additionally conferring specificity, while the volume of residues in the 261–268 loop also fine-tunes the enzyme catalytic efficiency (Catalano-Dupuy, et al. 2011, Hermoso, et al. 2002,

(For nomenclature and classification of FNR isoforms in different higher plant species, please see Mulo 2011)

Peregrina, et al. 2009, Sánchez-Azqueta, et al. 2014c, Tejero, et al. 2003). The loop allocating the FAD adenosine and a positively charged residue (R100 in AnFNR or K166 in $Spinacea\ oleracea$ FNR, SpFNR) at the FAD-binding domain address the NMN moiety of NADP$^+$ towards the active site (Aliverti, et al. 1991, Martínez-Júlvez, et al. 1998a, Peregrina, et al. 2009, Sánchez-Azqueta, et al. 2014c). These concerted changes bring the NMN moiety to a surface pocket near the isoalloxazine FAD cofactor (C-II in Fig. 3A and 3B). However, in this arrangement the stacking of the C-terminal Tyr (Y303 in AnFNR) against the re-face of the isoalloxazine ring blocks the approximation of the nicotinamide ring of the coenzyme to the flavin isoalloxazine ring.

It was proposed that the C-terminal Tyr had to be displaced to allow the nicotinamide entrance into the active site to approximate the C4N atom to the flavin N5 atom (Carrillo and Ceccarelli 2003, Hermoso, et al. 2002). Nevertheless, crystal structures with such an apparent productive rearrangement were only available for complexes in which the C-terminal Tyr was replaced with Ser or Trp (C-III in Fig. 3C and 3D) (Deng, et al. 1999, Tejero, et al. 2005). These mutants however produced large accumulation of CTC-2 when evaluating their ability to catalyze the photosynthetic reaction but were not able to evolve through HT to produce NADPH, while the reverse HT process was only slightly less efficient than for WT. These results therefore indicated that the C-terminal Tyr despite not being involved in the HT itself was surely critical for modulating the flavin midpoint potential and the NADP$^+$/H biding affinity and selectivity, as well as for the formation of the catalytically competent complex (Piubelli, et al. 2000, Tejero, et al. 2005). So far experimental methods have not provided a molecular image of the final architecture and relative orientation of the isoalloxazine, nicotinamide, and Tyr rings that allocates the C4N at adequate distance and orientation for HT to the N5 in the active site of the WT FNR HT competent complex (Carrillo and Ceccarelli 2003, Deng, et al. 1999, Hermoso, et al. 2002, Tejero, et al. 2005).

Fast kinetic methods have proven to be very efficient in the determination of the spectral properties of both CTCs and the corresponding interconversion HT rates (Peregrina, et al. 2010, Tejero, et al. 2007). An adequate initial interaction between the 2'P-AMP portion of NADP$^+$/H and FNR is critical for the subsequent conformational

(For nomenclature and classification of FNR isoforms in different higher plant species, please see Mulo 2011)

changes leading to CTC formation. Nevertheless, not strict correlation exits between the stability of the transient CTCs formation and the rate of the subsequent HT when analyzing different FNR mutants. The combined use of fast kinetic methods with kinetic isotope effects and the analysis of their temperature dependence reaction also provided a powerful tool to explore the dynamics of the FNR HT process (Lans, et al. 2010, Peregrina, et al. 2010, Sánchez-Azqueta, et al. 2014a). WT FNR evolved with active dynamics vibrational modulation of the active site narrowing the distance between the donor and acceptor atoms and enhancing the tunnel and the catalytic efficiency. The effect in donor-acceptor distance dynamics resulted larger in plant enzymes than in cyanobacterial ones, in agreement with previous experimental data indicating lower nicotinamide occupancy of the active site in the cyanobacterial enzymes (Aliverti, et al. 1995, Aliverti, et al. 1991, Nogués, et al. 2004, Sancho and Gómez-Moreno 1991, Sánchez-Azqueta, et al. 2014a). On the contrary, similar studies on bacterial FPRs were consistent with passive environmental reorganization movements dominating the HT coordinate and no contribution of donor-acceptor-donor sampling or gating fluctuations (Sánchez-Azqueta, et al. 2014a). This indicated that active sites of FPRs are more rigid than those for FNRs. Analysis of site-directed mutants in plastidic FNRs indicated in addition the requirement of a minimal optimal architecture in the catalytic complex to provide a favorable gating contribution, particularly in complexes of C-terminal residue mutants whose crystal structures predicted a close flavin:nicotinamide stacking. In these later cases the relative movement of the isoalloxazine and nicotinamide rings along the HT reaction coordinate was hardly allowed, indicating that the presence of the C-terminal Tyr has important thermodynamic and kinetic consequences in the overall process (Lans, et al. 2010, Peregrina, et al. 2010, Velázquez-Campoy, et al. 2006). In turn, application of the ensemble-averaged variational transition-state theory with multidimensional tunneling calculations using the crystal structure of the complex of $NADP^+$ with Y303S AnFNR provided reaction rate constants and kinetic isotope effects in agreement with experimental results. These calculations indicated that formation of a close contact ionic pair $FADH^-:NADP^+$ surrounded by the polar enzyme environment in the FNR_{hq}-$NADP^+$ reactant complex was the cause of the huge difference between the direct and

(For nomenclature and classification of FNR isoforms in different higher plant species, please see Mulo 2011)

the reverse reaction efficiencies (Lans, et al. 2010). Altogether these studies indicated that the architecture of the WT FNR active site and, particularly, the C-terminal Tyr side-chain organization contribute to reduce the stacking probability between the isoalloxazine and nicotinamide rings in the catalytically competent complexes, precisely modulating the angle and distance between the N5 and the C4N to values that ensure both reversibility and efficient HT processes.

Since WT FNR models for such architecture have not been elucidated by experimental methods, a molecular dynamics (MD) theoretical approach was used to model a putative organization at the active site of the transient catalytically competent interaction (Peregrina, et al. 2012). Such simulation produced theoretical structures for putative WT FNR_{hq}-$NADP^+$ and FNR_{ox}-NADPH catalytically competent complexes which allocated the C-terminal Tyr side-chain breaking the parallelism between the isoalloxazine and the nicotinamide rings and decreasing their mutual stacking, while keeping the reacting N5 and C4N atoms at a HT distance. Such control of the stacking was also shown to increase the N5-hydride–C4N angle and to produce a near co-linear disposition of the reacting atoms that will favor an efficient HT process (C-III* in Fig. 3A and 3B). These putative catalytically competent structures also showed stabilization of N4 and N7 atoms of the nicotinamide by key active site residues (S80, C261, and E301 in AnFNR and S90, C263 and E306 and in Pisum sativa FNR, PsFNR) (See Fig. 3 and 4 in (Peregrina, et al. 2012)). In addition, simulations show how the interaction with the ribose of the NMN moiety is improved by the dynamic displacement of the bulky residues in the 261–268 loop and how the 2'P-AMP binding cavity is narrowed to sandwich this coenzyme moiety between highly conserved Leu and Tyr residues.

Using the MD model structures for the complexes a fully microscopic simulation of the HT between FNR_{hq}/FNR_{ox} and $NADP^+$/H, also accounting for the solvation, was used to describe the potential energy surface of the whole system using a dual-level quantum mechanics/molecular mechanics (QM/MM) hybrid approach (Lans, et al. 2012). The results confirmed that the MD structural model of the reactants evolved to a catalytically competent transition state through very similar free energy barriers for both the forward and reverse reactions (See Fig. 6 in (Lans, et al. 2012)), in good agreement with the experimental HT rate constants reported for the system (Sánchez-

(For nomenclature and classification of FNR isoforms in different higher plant species, please see Mulo 2011)

Azqueta, et al. 2014a, Tejero, et al. 2007). This theoretical approach additionally provided subtle structural details of the mechanism in WT FNR and provided a structural explanation of why the C-terminal Tyr makes possible the photosynthetic reaction, a process that cannot occur when this Tyr is replaced by smaller residues (Lans, et al. 2010, Sánchez-Azqueta, et al. 2012, Tejero, et al. 2005). The presence of the C-terminal Tyr reduced the stacking probability between both rings and increased the collinearity between the reacting atoms, allowing arrangements compatible with HT.

2.3. The ternary complex.

As already indicated in early Batie and Kamin studies (Batie and Kamin 1984a, Batie and Kamin 1984b), nowadays it is fully accepted that ET from Fd to $NADP^+$ occurs through an ordered two-substrate process with the formation of at least two transient $Fd:FNR:NADP^+$ complexes (See Fig. 2 in (Carrillo and Ceccarelli 2003)). The process starts with the initial formation of $Fd_{rd}:FNR_{ox}:NADP^+$ complex that evolves to $Fd_{ox}:FNR_{sq}:NADP^+$, from which Fd_{ox} liberation has been identified as the rate limiting-step in the overall ET process. Release of Fd_{ox} will then allow the entrance of a second Fd_{rd} molecule to form the $Fd_{rd}:FNR_{sq}:NADP^+$ complex that will become the $Fd_{ox}:FNR_{hq}:NADP^+$ complex and from which HT from FNR_{hq} to $NADP^+$ will take place. Although such mechanism indicates that $NADP^+$ is able to occupy a site on FNR without displacing Fd (Batie and Kamin 1984a, Carrillo and Ceccarelli 2003, Hermoso, et al. 2002, Sancho and Gómez-Moreno 1991), ternary complexes show negative cooperativity and an increase in the enthalpic contribution (more favorable) and a decrease in the entropic contribution (less favorable), with regard to the binary complexes (Martínez-Júlvez, et al. 2009, Velázquez-Campoy, et al. 2006). Thus, the presence of Fd lowers the FNR affinity for $NADP^+$ and occupation of the $NADP^+$-binding site makes the Fd:FNR interaction weaker (Batie and Kamin 1984a, Martínez-Júlvez, et al. 2009, Velázquez-Campoy, et al. 2006). These facts therefore indicate that the Fd and $NADP^+$ binding sites on FNR are not completely independent. However, this negative cooperativity in the ternary interaction is translated into positive cooperativity at the kinetic level, since complex formation between Fd_{rd} and

14

(For nomenclature and classification of FNR isoforms in different higher plant species, please see Mulo 2011)

$FNR_{ox}:NADP^+$ increases the rate of ET by facilitating the rate-limiting dissociation of the Fd_{ox} product (Carrillo and Ceccarelli 2003, Hurley, et al. 2002, Medina 2009).

Despite efforts to obtain them, crystal structures of transient $Fd:FNR:NADP^+$ ternary complexes have not been achieved so far. Nevertheless, putative models were been produced on the bases of the crystal structures for binary Fd:FNR and $FNR:NADP^+$ interactions (See Fig. 4A in (Hermoso, et al. 2002)). These models confirmed that the $NADP^+$ binding site on FNR is not at the Fd:FNR interface, indicating that previous $NADP^+$ binding to FNR should not affect the protein-protein interaction. They also suggested that structural rearrangements in the $NADP^+$ binding domain of FNR (particularly in the 261–265 loop) upon coenzyme binding influence the conformation and orientation of residues involved not only in the productive Fd:FNR interaction for ET (See Fig. 4B in (Hermoso, et al. 2002)), but also in triggering Fd_{ox} release once ET is completed (Hurley, et al. 1993a, Morales, et al. 2000). Advance computational tools have not yet been used to simulate neither the formation of the ternary transitory $Fd:FNR:NADP^+$ complexes nor the ET and HT processes. Moreover, proton transfer associated to ET processes also remains to be investigated. It is envisaged that new atomistic information will be described in the coming years using as starting models the $Fd:FNR:NADP^+$ ternary complexes that can already been constructed on the bases of binary experimental and theoretical complexes (Fig. 4) together with the use of newly coming computational tools.

3.-Physiology of FNR

3.1 The diversity of FNR isoforms

The first apparent physiological question concerning chloroplast FNR isoforms is whether they play unique functional roles in metabolism. *Arabidopsis thaliana* (*At*FNRs) (Hanke, et al. 2005) and wheat (*Triticum aestivum, Ta*FNRs) contain two (Gummadova, et al. 2007), and maize three (*Zm*FNRs) (Okutani, et al. 2005) chloroplast FNR isoforms*, which may reflect the different metabolic demands of C3 and C4 photosynthesis. Although the *At*FNR isoforms share circa 80% sequence identity (Hanke, et al. 2005, Lintala, et al. 2009, Lintala, et al. 2007), they possess some unique properties. Under standard conditions the *AtFNR1* gene is expressed in higher levels than the *AtFNR2*, 68% of FNR transcripts representing *AtFNR1* (Lintala, et al. 2009). The

(For nomenclature and classification of FNR isoforms in different higher plant species, please see Mulo 2011)

expression of the *AtFNR2* gene, however, is induced by high nitrate concentrations, while that of *AtFNR1* is not (Hanke, et al. 2005) . Moreover, the *Atfnr2* knock-out plants show higher flexibility and somewhat better performance under low temperature conditions than *Atfnr1* (Lintala, et al. 2009). The most striking difference between the isoforms is evident only at molecular level, as the presence of *At*FNR1 isoform is required for membrane binding of *At*FNR2 (see 4.2; (Lintala, et al. 2007)). This finding is in line with the study of Hanke and collaborators (Hanke, et al. 2005) showing that *At*FNR1 is the most abundant form at the thylakoid membrane, while *At*FNR2 is mostly present in the soluble stroma. Additionally, both *At*FNR isoforms are targets of multiple post-translational modifications (PTMs), including alternative processing of the N-termini, N-terminal as well as Lys-acetylation (Lehtimäki, et al. 2014). Both isoforms (*At*FNR1 and *At*FNR2) exist as two distinct spots after 2-D gel electrophoresis, the more acidic spot representing N-terminally acetylated form of the enzyme (Lehtimäki, et al. 2014). Although the physiological significance of the N-terminal acetylation is not yet known, it is important to note that the ratio of N-terminally acetylated:non-acetylated FNR isoforms changes upon dark-light shifts (Lehtimäki, et al. 2014). As one of the conserved Lys residues modified by acetylation is located in a close proximity to the catalytic site of the enzyme (in both isoforms), it is conceivable that the PTMs might affect the activity of FNR (Lehtimäki, et al. 2014) .

In wheat more detailed information about the specificity of FNR isoforms is available. The unprocessed *Ta*FNRII isoform showed higher catalytic activity, but lower affinity to Fd than the unprocessed *Ta*FNRI (Gummadova, et al. 2007). N-terminal processing of *Ta*FNRI and *Ta*FNRII leads to differences in function: truncation of the *Ta*FNRI N-termini by two to three amino acids resulted in decreased activity without any effect on Fd affinity (Gummadova, et al. 2007). In contrast, the unprocessed form of *Ta*FNRII was able to distinguish between the different Fd isoforms, but upon truncation of the N-terminus the discrimination capacity was lost (Bowsher, et al. 2011, Gummadova, et al. 2007). Additionally, accumulation of differently processed *Ta*FNRI responded to changes in developmental stage of the leaf and nitrogen regime, as well as upon challenging with methyl viologen (Moolna and Bowsher 2010). Processing of the N-termini also affected distribution of *Ta*FNRI between the soluble

(For nomenclature and classification of FNR isoforms in different higher plant species, please see Mulo 2011)

and thylakoid pool (Moolna and Bowsher 2010). Also the N-termini of the three leaf-type FNR isoforms identified in maize affects the subchloroplastic location of each form (Okutani, et al. 2005, Twachtmann, et al. 2012). In general, ZmFNR1 is bound to the thylakoids and ZmFNR3 exists in a soluble form, while ZmFNR2 has a dual location (Okutani, et al. 2005). The distribution of the isoforms between the cell types (mesophyll $vs.$ bundle sheath) reflects the metabolic needs of a given tissue. The soluble ZmFNR2 and ZmFNR3 are found in the mesophyll cells, predominantly performing linear PET, while the membrane-bound isoforms ZmFNR1 and ZmFNR2 are abundant in the bundle sheath cells known to conduct CET (Twachtmann, et al. 2012). It is also worth noting that the catalytic activities of ZmFNR2 and ZmFNR3 were higher than that of ZmFNR1, and that the isoforms showed unique properties in the formation of the Fd:FNR complex in response to changes in pH and on the dependence of specific intermolecular salt bridges (Okutani et al. 2005).

3.2 Dynamic allocation of FNR

The physiological significance of FNR distribution between the soluble and membrane-bound pools has puzzled plant scientists for decades. It has been shown that the photoreduction activity of $NADP^+$ is much higher for membrane-bound than for soluble FNR (Forti and Bracale 1984), and that the soluble FNR cannot complement the $NADP^+$ photoreduction activity of mutant thylakoid membrane devoid of FNR (Hanke, et al. 2008). However, as the Arabidopsis mutant plants lacking membrane-bound FNR do not show drastic visual phenotype or marked deficiencies in photosynthetic reactions (Benz, et al. 2009, Hanke, et al. 2008, Lintala, et al. 2007, Lintala, et al. 2012, Yang, et al. 2016), it seems plausible that also the soluble FNR can support autotrophic growth of the plants.

Moreover, the site, mechanism and functional consequences of membrane binding have been under debate for a long time (for a review, see (Mulo 2011)). Earlier, membrane tethering of FNR was suggested to occur via specific FNR binding proteins, such as base protein (Chan, et al. 1987, Pessino, et al. 1994, Soncini and Vallejos 1989, Vallejos, et al. 1984) or connectein (Shin, et al. 1985, Shin, et al. 1990). FNR has also been indicated in interaction with PSI (Andersen, et al. 1992), NDH complex (Guedeney, et al. 1996, Quiles and Cuello 1998) as well as Cytochrome b_6f

(For nomenclature and classification of FNR isoforms in different higher plant species, please see Mulo 2011)

complex (Clark, et al. 1984, Zhang, et al. 2001) (Fig. 5). Although *Sp*FNR, as well as *Zm*FNR1 and *Zm*FNR2 (but not *Zm*FNR3), have been shown to copurify with the Cyt b$_6$f complex (Clark, et al. 1984, Okutani, et al. 2005, Zhang, et al. 2001), a novel Tic62 and/or Trol dependent mechanism was recently revealed to be responsible for membrane binding of FNR in Arabidopsis (Benz, et al. 2009, Jurić, et al. 2009), and later for maize (Twachtmann, et al. 2012) and rice (Yang, et al. 2016). Tic62 is a 62 kDa protein originally identified as an extrinsic subunit of the Tic (Translocon of Inner Chloroplast membrane) complex, which was shown to interact with FNR (Balsera, et al. 2007, Küchler, et al. 2002). It was also shown that Tic62 exists as a soluble protein in stroma (Stengel, et al. 2008), and that it accumulates in high molecular weight protein complexes at the thylakoid membrane together with FNR (Benz, et al. 2009). Accumulation of these complexes is highly dynamic and dependent on light: accumulation of protein complexes takes place in darkness, while increase in illumination results in disassembly of complexes and release of FNR from the membrane. Similarly, the integral thylakoid membrane protein Trol (Thylakoid Rhodanase Like protein) forms a high molecular weight complex together with FNR (Jurić, et al. 2009). Intriguingly, Tic62 and Trol contain one or more serine/proline –rich motifs in their C-termini, which have been shown to bind FNR (Alte, et al. 2010, Balsera, et al. 2007, Benz, et al. 2010). This domain is present only in Tic62 protein of vascular plants (Balsera, et al. 2007), but also the C4 plants maize and *Sorghum bicolor* seem to lack it (Twachtmann, et al. 2012). These differences indicate variation in the membrane tethering mechanisms of FNR depending on the physiological properties of a given organism. These differences may be exemplified by the unicellular cyanobacterium *Synechocystis* sp. PCC6803, which lacks the Tic62 protein and binds FNR to the phycobilisome via an extension in the N-terminus of FNR (Thomas, et al. 2006).

Recently, a novel component of the FNR-containing protein complexes in higher plants was described. The LIR1 (Light Induced Rice1) protein interacts with FNR and accumulates in FNR-containing thylakoid protein complexes (Yang, et al. 2016). Indeed, the rapid light-dependent degradation of the LIR1 protein coinciding with the disassembly of the FNR-containing protein complexes might provide a mechanism for

(For nomenclature and classification of FNR isoforms in different higher plant species, please see Mulo 2011)

regulation of FNR (re)allocation between the soluble and membrane pools within the chloroplast (Yang, et al. 2016).

3.3 Physiological impacts of the FNR action

Despite numerous studies, our understanding of the functional specificity of distinct FNR isoforms and physiological significance of FNR distribution between soluble and membrane fractions is still insufficient. Obviously, FNR is essential for linear electron flow and plant survival (Lintala, et al. 2012), but there is plenty of contradictory data concerning the role of FNR in CET. In maize, the distribution of specific FNR isoforms between the mesophyll and bundle sheath cells indicates unique functional properties required for C3 or C4 photosynthesis, but it is not clear whether this specificity originates from the structural and/or catalytic differences of the isoforms, or is it rather due to differential subchloroplastic location (Twachtmann, et al. 2012). The situation is even more complicated in C3 plants, in which the pathways and regulation of CET is still under debate (Suorsa 2015). The presence of FNR in the close proximity to Cyt b_6f complex (Clark, et al. 1984, Zhang, et al. 2001) and to the other components of Fd-dependent CET (DalCorso, et al. 2008), ET from FNR to quinones (Bojko et al. 2003) as well as FNR inhibitors disrupting cyclic electron flow (Shahak, et al. 1981) have prompted suggestions of FNR being involved in CET.

FNR has also been implicated in the responses to oxidative stress. Firstly, expression of a *Ps*FNR gene in methyl viologen sensitive, FNR deficient strain of *Escherichia coli* restored the tolerance of bacteria to oxidative stress (Krapp, et al. 2002). In line with these studies, over-expression of FNR in tobacco (*Nicotiana tabacum*) plants increased the tolerance against oxidative stress (Rodriguez, et al. 2007), while the decrease of chloroplast FNR amount leads to chlorosis, reduced growth and oxidative stress of the plants (Lintala, et al. 2009, Lintala, et al. 2007, Palatnik, et al. 2003). It has also been shown that oxidative stress, propagated either by exposure of the plant to methyl viologen (Palatnik, et al. 1997) or to intense illumination (Benz, et al. 2009) or water stress (Lehtimäki, et al. 2010), leads to release of FNR from the thylakoid membrane. This, again, raises the question about the effect of subchloroplastic location on the regulation of FNR function (see 3.2).

(For nomenclature and classification of FNR isoforms in different higher plant species, please see Mulo 2011)

Another important but poorly understood aspect is the role of FNR in the dark metabolism of chloroplasts. It is assumed that during the dark periods FNR oxidizes NADPH, originating from pentose phosphate pathway, and reduces Fd which then provides reducing power to the assimilation on nitrogen and sulfur. Due to methodological difficulties it has been challenging to measure the FNR activity *in planta* and to determine the physiological conditions and molecular factors regulating the function of FNR in darkness. For instance, it will be interesting to reveal whether the specific isoforms of FNR and/or Fd are primarily used under heterotrophic conditions.

4.-Concluding remarks and perspectives

Despite marked progress during the past decades in understanding the structure-function relationships behind the kinetics of the ET and HT process involving FNR as well as the physiological properties of FNR, there are still numerous fundamental open questions about the regulation of the FNR function. For instance, future research is required to reveal the main molecular intermediates and final species of the equilibrium mixture in the ET and HT processes within competent ternary complexes, and the contribution of proton transfer coupled to the efficiency of ET between Fd and FNR in binary and ternary complexes. We also do not know yet how does the presence of Fd modulate HT among FNR and the coenzyme, or how does the presence of the coenzyme modulate the interaction and ET among Fd and FNR at the atomistic, molecular and dynamic levels. Furthermore, the functional roles of soluble and membrane-bound FNR pools, the unique functional properties of the distinct FNR isoforms and the functional determinants of FNR activity upon various conditions remain to be elucidated. It is likely that future research will provide further knowledge and detailed mechanisms for the Fd:FNR:NADP(H) complexation as well as for the electron and proton exchange processes involving FNR. As these reactions are of utmost importance for the plant productivity, answers to these questions will be useful for biotechnological engineering of plants and algae towards sustainable production of food and energy for the mankind.

Figure Legends.

(For nomenclature and classification of FNR isoforms in different higher plant species, please see Mulo 2011)

Figure 1. *An*FNR and *An*Fd crystal structures. (A) Molecular surface and cartoon representation of *An*FNR (PDB CODE: 1que). Binding domains for each cofactor, FAD and NADP$^+$, are colored in pale pink and in metallic violet, respectively. (B) Detail of the *An*FNR active center showing in CPK colored sticks key residues. (C) Molecular surface with the electrostatic potential of *An*FNR at the ligands binding environment. Positions of key residues for the Fd interaction are highlighted. In all cases FAD is represented in CPK sticks with carbons colored orange. (D) Cartoon representation of *An*Fd in oxidized and reduced state (PDB CODE: 1czp). (E) Detail of the environment of the *An*Fd [2Fe-2S] redox center. The C46-C47 and C47-C48 peptide bonds are highlighted as sticks CPK colored with carbons in green and grey respectively for the Fd$_{ox}$ and Fd$_{rd}$ redox states. The [2Fe-2S] and cysteine residues binding it are shown in sticks. Key residues for the interaction with FNR are shown in sticks and CPK colored with carbons in blue. (F) Molecular surface with the electrostatic potential of *An*Fd at the FNR binding environment. Positions of key residues for the FNR interaction are highlighted. Figure produced using PyMOL (Delano 2002).

Figure 2. Structural models for the Fd:FNR complex. Cartoon representation of (A) the crystallographic complex in *Zea mays* (PDB CODE: 1gaq), (B) the crystallographic complex in *Anabaena* (PDB CODE: 1ewy) and (C) superimposition of the 20 lowest energy structures from a coarse-grained protein–protein docking followed by all-atom refinement (Saen-Oon, et al. 2015). FNR binding domains for FAD and NADP$^+$ are colored in pale pink and metallic violet respectively. *Zm*Fd is colored in pale magenta and *An*Fd in magenta. FNR key residues for Fd binding at the FAD binding domain and key catalytic residues at the C-terminal are shown as sticks with carbons in beige and lemon respectively. The loop 37-47 in *Zm*Fd and the loop 39–49 in *An*Fd are colored in light blue. The side chain of F65 *An*Fd is shown in dark blue for each of the predicted Fd conformation in (C). Fd orientation regarding FNR rotates when comparing *Zm* and *An* crystallographic complexes. Nevertheless, both conformations might be included between the different docking predicted conformations. This suggests more than one orientation might bring redox centers to adequate distance and orientation for ET. In all cases FAD is represented in CPK sticks with carbons colored orange and the [2Fe-2S] cluster in spheres with Fe and sulfur in orange and yellow respectively.

21

(For nomenclature and classification of FNR isoforms in different higher plant species, please see Mulo 2011)

Figure 4. Structural conformations proposed for the different steps in the interaction of *An*FNR with the coenzyme to attain the catalytically competent complex for HT. (A) Relative disposition of the isoalloxazine and the coenzyme with regard to the protein surface and (B) detail of the isoalloxazine-nicotinamide structural relationships for the different complexes. C-1, crystallographic FNR_{ox}:$NADP^+$ obtained by soaking, (PDB CODE 1quf), related with the initial recognition of the 2-P-AMP moiety of $NADP^+$ by FNR (Serre, et al. 1996). C-II, crystallographic FNR_{ox}:$NADP^+$ (PDB CODE 1gjr) showing the narrowing of the 2-P-AMP and the PPi binding cavity with Y303 preventing stacking of the nicotinamide against the isoalloxazine ring (Hermoso, et al. 2002). C-III*, equilibrium molecular dynamics conformation representing a putative catalytically competent WT FNR_{ox}:NADPH CTC complex in which the Y303 situates its hydroxyl between the N10 of the isoalloxazine and the N1N of the nicotinamide helping to provide a favorable orientation (almost co-linear) among the N5 acceptor, the hydride to be transferred and the C4N donor while preventing a close non-productive stacking between the reacting rings (a similar organization is predicted for the FNR_{hq}:$NADP^+$ CTC structure when similarly analyzed) (Peregrina, et al. 2012). These MD FNR_{hq}:$NADP^+$ and FNR_{ox}:NADPH C-III* structures show the simultaneous allocation in the isoalloxazine active site environment of the nicotinamide and the Y303 and when evaluating their HT efficiency resulted compatible with experimental data (Lans, et al. 2012). (C) Isoalloxazine and coenzyme disposition with regard to the protein surface and (B) detail of the isoalloxazine-nicotinamide coupling in the crystallographic structure of the Y303S FNR_{ox}:$NADP^+$ complex (PDB CODE: 2bsa) showing a close isoalloxazine-nicotinamide stacking that prevents reaction in the photosynthetic direction (Lans, et al. 2010, Tejero, et al. 2005). In all cases FAD and $NADP^+$/H are represented in CPK sticks with carbons colored orange and green respectively. The C-terminal residue (Y303 or S303) is shown in CPK with carbons in lime green.

Figure 5. Possible models for transient Fd:FNR:$NADP^+$ ternary complexes in *Anabaena*. (A) Model obtained by superposition of FNR coordinates in the crystallographic Fd:FNR (PDB CODE: 1ewy) complex (Morales, et al. 2000) with FNR coordinates in a theoretical FNR:$NADP^+$ complex compatible with efficient HT from N5 to C4N (Lans, et al. 2012, Peregrina, et al. 2012). Fd from the crystallographic complex and FNR from the

(For nomenclature and classification of FNR isoforms in different higher plant species, please see Mulo 2011)

theoretical one are shown as magenta and grey, respectively, transparent molecular surfaces. The inset shows a detail of the active site in the ternary complexes with the flow of electrons and hydride in the photosynthetic direction. (B) Model obtained by superposition of FNR coordinates in a theoretical FNR:NADP$^+$ complex compatible with efficient HT from N5 to C4N (Lans, et al. 2012, Peregrina, et al. 2012) with FNR coordinates in one of the 20 lowest energy structures from a coarse-grained protein–protein docking followed by all-atom refinement (Saen-Oon, et al. 2015). The 20 lowest energy positions for Fd are represented as in Fig. 2C, while FNR from the theoretical FNR:NADP$^+$ complex is shown in grey molecular surface. In all cases, the FAD and NADP$^+$ are shown in sticks with carbons in orange and green respectively. Position of the C-terminal Tyr is shown in lemon color.

Figure 5. A simplified scheme of photosynthetic ET reactions. Electrons abstracted from water are transferred via Photosystem II (PSII), Cytochrome b_6f complex (Cyt b_6f), plastocyanin (PC) and Photosystem I (PSI) to ferredoxin (Fd). Two independent Fd molecules provide reducing power to FNR for the production of NADPH. Apparently both the soluble FNR and the membrane-bound FNR, interacting with the Tic62, LIR1 and Trol proteins, are active in the photoreduction of NADP$^+$. In addition to linear electron transfer, electrons may be circulated around PSI either via the NDH-dependent pathway (1) or the Fd-dependent pathway (2). See text for details.

(For nomenclature and classification of FNR isoforms in different higher plant species, please see Mulo 2011)

REFERENCES

Aliverti A, Bruns CM, Pandini VE, Karplus PA, Vanoni MA, Curti B, Zanetti G (1995) Involvement of serine 96 in the catalytic mechanism of ferredoxin-NADP+ reductase: structure-function relationship as studied by site-directed mutagenesis and X-ray crystallography. Biochemistry 34: 8371-8379 doi:

Aliverti A, Corrado ME, Zanetti G (1994) Involvement of lysine-88 of spinach ferredoxin-NADP+ reductase in the interaction with ferredoxin. FEBS Lett 343: 247-250 doi: 0014-5793(94)80565-2 [pii]

Aliverti A, Deng Z, Ravasi D, Piubelli L, Karplus PA, Zanetti G (1998) Probing the function of the invariant glutamyl residue 312 in spinach ferredoxin-NADP+ reductase. J Biol Chem 273: 34008-34015 doi:

Aliverti A, Faber R, Finnerty CM, Ferioli C, Pandini V, Negri A, Karplus PA, Zanetti G (2001) Biochemical and crystallographic characterization of ferredoxin-NADP+ reductase from nonphotosynthetic tissues. Biochemistry 40: 14501-14508 doi: bi011224c [pii]

Aliverti A, Lubberstedt T, Zanetti G, Herrmann RG, Curti B (1991) Probing the role of lysine 116 and lysine 244 in the spinach ferredoxin-NADP+ reductase by site-directed mutagenesis. J Biol Chem 266: 17760-17763 doi:

Aliverti A, Pandini V, Pennati A, de Rosa M, Zanetti G (2008) Structural and functional diversity of ferredoxin-NADP+ reductases. Arch Biochem Biophys 474: 283-291 doi: S0003-9861(08)00076-3 [pii] 10.1016/j.abb.2008.02.014

Aliverti A, Piubelli L, Zanetti G, Lubberstedt T, Herrmann RG, Curti B (1993) The role of cysteine residues of spinach ferredoxin-NADP+ reductase as assessed by site-directed mutagenesis. Biochemistry 32: 6374-6380 doi:

Alte F, Stengel A, Benz JP, Petersen E, Soll J, Groll M, Bölter B (2010) Ferredoxin:NADPH oxidoreductase is recruited to thylakoids by binding to a polyproline type II helix in a pH-dependent manner. Proc Natl Acad Sci U S A 107: 19260-19265 doi: 10.1073/pnas.1009124107

Andersen B, Scheller HV, Møller BL (1992) The PSI-E subunit of photosystem I binds ferredoxin:NADP+ oxidoreductase. FEBS Lett 311: 169-173 doi:

Arakaki AK, Ceccarelli EA, Carrillo N (1997) Plant-type ferredoxin-NADP+ reductases: a basal structural framework and a multiplicity of functions. FASEB J 11: 133-140 doi:

Arakaki AK, Orellano EG, Calcaterra NB, Ottado J, Ceccarelli EA (2001) Involvement of the flavin si-face tyrosine on the structure and function of ferredoxin-NADP+ reductases. J Biol Chem 276: 44419-44426 doi: 10.1074/jbc.M107568200 M107568200 [pii]

Arnon DI (1991) Photosynthetic electron transport: Emergence of a concept, 1949-59. Photosynth Res 29: 117-131 doi: 10.1007/BF00036216

Arnon DI, Chain RK (1975) Regulation of ferredoxin-catalyzed photosynthetic phosphorylations. Proc Natl Acad Sci U S A 72: 4961-4965 doi:

Balsera M, Stengel A, Soll J, Bölter B (2007) Tic62: a protein family from metabolism to protein translocation. BMC Evol Biol 7: 43 doi: 10.1186/1471-2148-7-43

Batie CJ, Kamin H (1984a) Electron transfer by ferredoxin:NADP+ reductase. Rapid-reaction evidence for participation of a ternary complex. J Biol Chem 259: 11976-11985 doi:

Batie CJ, Kamin H (1984b) Ferredoxin:NADP+ oxidoreductase. Equilibria in binary and ternary complexes with NADP+ and ferredoxin. J Biol Chem 259: 8832-8839 doi:

Batie CJ, Kamin H (1986) Association of ferredoxin-NADP+ reductase with NADP(H) specificity and oxidation-reduction properties. J Biol Chem 261: 11214-11223 doi:

Benz JP, Lintala M, Soll J, Mulo P, Bölter B (2010) A new concept for ferredoxin-NADP(H) oxidoreductase binding to plant thylakoids. Trends Plant Sci 15: 608-613 doi: 10.1016/j.tplants.2010.08.008

(For nomenclature and classification of FNR isoforms in different higher plant species, please see Mulo 2011)

Benz JP, Stengel A, Lintala M, Lee YH, Weber A, Philippar K, Gügel IL, Kaieda S, Ikegami T, Mulo P, Soll J, Bölter B (2009) Arabidopsis Tic62 and ferredoxin-NADP(H) oxidoreductase form light-regulated complexes that are integrated into the chloroplast redox poise. Plant Cell 21: 3965-3983 doi: 10.1105/tpc.109.069815

Bhattacharyya AK, Meyer TE, Cusanovich MA, Tollin G (1987) Laser flash photolysis studies of electron transfer between ferredoxin-NADP+ reductase and several high-potential redox proteins. Biochemistry 26: 758-764 doi:

Bowsher CG, Eyres LM, Gummadova JO, Hothi P, McLean KJ, Munro AW, Scrutton NS, Hanke GT, Sakakibara Y, Hase T (2011) Identification of N-terminal regions of wheat leaf ferredoxin NADP+ oxidoreductase important for interactions with ferredoxin. Biochemistry 50: 1778-1787 doi: 10.1021/bi1014562

Bruns CM, Karplus PA (1995) Refined crystal structure of spinach ferredoxin reductase at 1.7 Å resolution: oxidized, reduced and 2'-phospho-5'-AMP bound states. J Mol Biol 247: 125-145 doi: S0022283684701276 [pii]

Carrillo N, Ceccarelli EA (2003) Open questions in ferredoxin-NADP+ reductase catalytic mechanism. Eur J Biochem 270: 1900-1915 doi: 3566 [pii]

Cassan N, Lagoutte B, Sétif P (2005) Ferredoxin-NADP+ reductase. Kinetics of electron transfer, transient intermediates, and catalytic activities studied by flash-absorption spectroscopy with isolated photosystem I and ferredoxin. J Biol Chem 280: 25960-25972 doi: 10.1074/jbc.M503742200

Catalano-Dupuy DL, Musumeci MA, Lopez-Rivero A, Ceccarelli EA (2011) A highly stable plastidic-type ferredoxin-NADP(H) reductase in the pathogenic bacterium Leptospira interrogans. PLoS One 6: e26736 doi: 10.1371/journal.pone.0026736 PONE-D-11-07131 [pii]

Ceccarelli EA, Arakaki AK, Cortez N, Carrillo N (2004) Functional plasticity and catalytic efficiency in plant and bacterial ferredoxin-NADP(H) reductases. Biochim Biophys Acta 1698: 155-165 doi: 10.1016/j.bbapap.2003.12.005 S1570963903003923 [pii]

Chan RL, Ceccarelli EA, Vallejos RH (1987) Immunological studies of the binding protein for chloroplast ferredoxin-NADP+ reductase. Arch Biochem Biophys 253: 56-61 doi:

Clark RD, Hawkesford MJ, Coughlan SJ, Bennett J, Hind G (1984) Association of Ferredoxin-NADP+ oxidoreductase with the chloroplast Cytochrome B-F Complex. FEBS Lett., pp. 137-142.

Corrado ME, Aliverti A, Zanetti G, Mayhew SG (1996) Analysis of the oxidation-reduction potentials of recombinant ferredoxin-NADP+ reductase from spinach chloroplasts. Eur J Biochem 239: 662-667 doi:

DalCorso G, Pesaresi P, Masiero S, Aseeva E, Schünemann D, Finazzi G, Joliot P, Barbato R, Leister D (2008) A complex containing PGRL1 and PGR5 is involved in the switch between linear and cyclic electron flow in Arabidopsis. Cell 132: 273-285 doi: 10.1016/j.cell.2007.12.028

Delano WL (2002) They PyMOL molecular graphics system. DeLano Scientific, San Carlos, CA, USA: http://www.pymol.org doi:

Deng Z, Aliverti A, Zanetti G, Arakaki AK, Ottado J, Orellano EG, Calcaterra NB, Ceccarelli EA, Carrillo N, Karplus PA (1999) A productive NADP+ binding mode of ferredoxin-NADP+ reductase revealed by protein engineering and crystallographic studies. Nat Struct Biol 6: 847-853 doi: 10.1038/12307

Dorowski A, Hofmann A, Steegborn C, Boicu M, Huber R (2001) Crystal structure of paprika ferredoxin-NADP+ reductase. Implications for the electron transfer pathway. J Biol Chem 276: 9253-9263 doi: 10.1074/jbc.M004576200 M004576200 [pii]

(For nomenclature and classification of FNR isoforms in different higher plant species, please see Mulo 2011)

Faro M, Frago S, Mayoral T, Hermoso JA, Sanz-Aparicio J, Gomez-Moreno C, Medina M (2002a) Probing the role of glutamic acid 139 of Anabaena ferredoxin-NADP+ reductase in the interaction with substrates. Eur J Biochem 269: 4938-4947 doi: 3194 [pii]

Faro M, Gomez-Moreno C, Stankovich M, Medina M (2002b) Role of critical charged residues in reduction potential modulation of ferredoxin-NADP+ reductase. Eur J Biochem 269: 2656-2661 doi: 2925 [pii]

Forti G, Bracale M (1984) Ferredoxin-ferredoxin NADP+ reductase interaction. FEBS Lett., pp. 81-84.

Foust GP, Mayhew SG, Massey V (1969) Complex formation between ferredoxin triphosphopyridine nucleotide reductase and electron transfer proteins. J Biol Chem 244: 964-970 doi:

Fredricks WW, Gehl JM (1982) Kinetics of extraction of ferredoxin-nicotinamide adenine dinucleotide phosphate reductase from spinach chloroplasts. Arch Biochem Biophys 213: 67-72 doi:

Goss T, Hanke G (2014) The end of the line: can ferredoxin and ferredoxin NADP(H) oxidoreductase determine the fate of photosynthetic electrons? Curr Protein Pept Sci 15: 385-393 doi:

Green LS, Yee BC, Buchanan BB, Kamide K, Sanada Y, Wada K (1991) Ferredoxin and ferredoxin-NADP reductase from photosynthetic and nonphotosynthetic tissues of tomato. Plant Physiol 96: 1207-1213 doi:

Grzyb J, Malec P, Rumak I, Garstka M, Strzałka K (2008) Two isoforms of ferredoxin:NADP(+) oxidoreductase from wheat leaves: purification and initial biochemical characterization. Photosynth Res 96: 99-112 doi: 10.1007/s11120-008-9289-y

Guedeney G, Corneille S, Cuiné S, Peltier G (1996) Evidence for an association of ndh B, ndh J gene products and ferredoxin-NADP-reductase as components of a chloroplastic NAD(P)H dehydrogenase complex. FEBS Lett 378: 277-280 doi:

Gummadova JO, Fletcher GJ, Moolna A, Hanke GT, Hase T, Bowsher CG (2007) Expression of multiple forms of ferredoxin NADP+ oxidoreductase in wheat leaves. J Exp Bot 58: 3971-3985 doi: erm252 [pii] 10.1093/jxb/erm252

Hanke G, Mulo P (2013) Plant type ferredoxins and ferredoxin-dependent metabolism. Plant Cell Environ 36: 1071-1084 doi: 10.1111/pce.12046

Hanke G, Okutani S, Satomi Y, Takao T, Suzuki, Hase T (2005) Multiple iso-proteins of FNR in Arabidopsis: evidence for different contributions to chloroplast function and nitrogen assimilation. *Plant, Cell & Environment*Plant, Cell & Environment, pp. 1146-1157.

Hanke GT, Endo T, Satoh F, Hase T (2008) Altered photosynthetic electron channelling into cyclic electron flow and nitrite assimilation in a mutant of ferredoxin:NADP(H) reductase. Plant Cell Environ 31: 1017-1028 doi: 10.1111/j.1365-3040.2008.01814.x

Hermoso JA, Mayoral T, Faro M, Gomez-Moreno C, Sanz-Aparicio J, Medina M (2002) Mechanism of coenzyme recognition and binding revealed by crystal structure analysis of ferredoxin-NADP+ reductase complexed with NADP+. J Mol Biol 319: 1133-1142 doi: 10.1016/S0022-2836(02)00388-1 S0022-2836(02)00388-1 [pii]

Hurley J, Cheng H, Xia B, Markley J, Medina M, Gomez-Moreno C, Tollin G (1993a) An aromatic amino acid is required at position 65 in Anabaena ferredoxin for rapid electron transfer to ferredoxin:NADP+ reductase. Journal of the American Chemical Society 115: 11698-11701 doi: 10.1021/ja00078a006

Hurley JK, Faro M, Brodie TB, Hazzard JT, Medina M, Gómez-Moreno C, Tollin G (2000) Highly nonproductive complexes with Anabaena ferredoxin at low ionic strength are induced by nonconservative amino acid substitutions at Glu139 in Anabaena ferredoxin:NADP+ reductase. Biochemistry 39: 13695-13702 doi:

(For nomenclature and classification of FNR isoforms in different higher plant species, please see Mulo 2011)

Hurley JK, Hazzard JT, Martínez-Júlvez M, Medina M, Gómez-Moreno C, Tollin G (1999) Electrostatic forces involved in orienting Anabaena ferredoxin during binding to Anabaena ferredoxin:NADP+ reductase: site-specific mutagenesis, transient kinetic measurements, and electrostatic surface potentials. Protein Sci 8: 1614-1622 doi: 10.1110/ps.8.8.1614

Hurley JK, Medina M, Gomez-Moreno C, Tollin G (1994) Further characterization by site-directed mutagenesis of the protein-protein interface in the ferredoxin/ferredoxin:NADP+ reductase system from Anabaena: requirement of a negative charge at position 94 in ferredoxin for rapid electron transfer. Arch Biochem Biophys 312: 480-486 doi:

Hurley JK, Morales R, Martínez-Júlvez M, Brodie TB, Medina M, Gómez-Moreno C, Tollin G (2002) Structure-function relationships in Anabaena ferredoxin/ferredoxin-NADP+ reductase electron transfer: insights from site-directed mutagenesis, transient absorption spectroscopy and X-ray crystallography. Biochim Biophys Acta 1554: 5-21 doi:

Hurley JK, Salamon Z, Meyer TE, Fitch JC, Cusanovich MA, Markley JL, Cheng H, Xia B, Chae YK, Medina M, et al. (1993b) Amino acid residues in Anabaena ferredoxin crucial to interaction with ferredoxin-NADP+ reductase: site-directed mutagenesis and laser flash photolysis. Biochemistry 32: 9346-9354 doi:

Hurley JK, Schmeits JL, Genzor C, Gómez-Moreno C, Tollin G (1996) Charge reversal mutations in a conserved acidic patch in Anabaena ferredoxin can attenuate or enhance electron transfer to ferredoxin:NADP+ reductase by altering protein/protein orientation within the intermediate complex. Arch Biochem Biophys 333: 243-250 doi: S0003-9861(96)90387-2 [pii] 10.1006/abbi.1996.0387

Hurley JK, Weber-Main AM, Stankovich MT, Benning MM, Thoden JB, Vanhooke JL, Holden HM, Chae YK, Xia B, Cheng H, Markley JL, Martínez-Júlvez M, Gómez-Moreno C, Schmeits JL, Tollin G (1997) Structure-function relationships in Anabaena ferredoxin: correlations between X-ray crystal structures, reduction potentials, and rate constants of electron transfer to ferredoxin:NADP+ reductase for site-specific ferredoxin mutants. Biochemistry 36: 11100-11117 doi:

Iwai M, Takizawa K, Tokutsu R, Okamuro A, Takahashi Y, Minagawa J (2010) Isolation of the elusive supercomplex that drives cyclic electron flow in photosynthesis. Nature 464: 1210-1213 doi: 10.1038/nature08885

Jelesarov I, Bosshard HR (1994) Thermodynamics of ferredoxin binding to ferredoxin:NADP+ reductase and the role of water at the complex interface. Biochemistry 33: 13321-13328 doi:

Jelesarov I, De Pascalis AR, Koppenol WH, Hirasawa M, Knaff DB, Bosshard HR (1993) Ferredoxin binding site on ferredoxin: NADP+ reductase. Differential chemical modification of free and ferredoxin-bound enzyme. Eur J Biochem 216: 57-66 doi:

Joliot P, Joliot A (2002) Cyclic electron transfer in plant leaf. Proc Natl Acad Sci U S A 99: 10209-10214 doi: 10.1073/pnas.102306999

Jurić S, Hazler-Pilepić K, Tomasić A, Lepedus H, Jelicić B, Puthiyaveetil S, Bionda T, Vojta L, Allen JF, Schleiff E, Fulgosi H (2009) Tethering of ferredoxin:NADP+ oxidoreductase to thylakoid membranes is mediated by novel chloroplast protein TROL. Plant J 60: 783-794 doi: 10.1111/j.1365-313X.2009.03999.x

Karplus PA, Daniels MJ, Herriott JR (1991) Atomic structure of ferredoxin-NADP+ reductase: prototype for a structurally novel flavoenzyme family. Science 251: 60-66 doi:

Khruschev SS, Abaturova AM, Diakonova AN, Fedorov VA, Ustinin DM, Kovalenko IB, Riznichenko GY, Rubin AB (2015) [Brownian dynamics simulations of protein-protein interactions in photosynthetic electron transport chain]. Biofizika 60: 270-292 doi:

(For nomenclature and classification of FNR isoforms in different higher plant species, please see Mulo 2011)

Kinoshita M, Kim JY, Kume S, Sakakibara Y, Sugiki T, Kojima C, Kurisu G, Ikegami T, Hase T, Kimata-Ariga Y, Lee YH (2015) Physicochemical nature of interfaces controlling ferredoxin NADP(+) reductase activity through its interprotein interactions with ferredoxin. Biochim Biophys Acta 1847: 1200-1211 doi: 10.1016/j.bbabio.2015.05.023

Krapp AR, Rodríguez RE, Poli HO, Paladini DH, Palatnik JF, Carrillo N (2002) The flavoenzyme ferredoxin (flavodoxin)-NADP(H) reductase modulates NADP(H) homeostasis during the soxRS response of Escherichia coli. J Bacteriol 184: 1474-1480 doi:

Kurisu G, Kusunoki M, Katoh E, Yamazaki T, Teshima K, Onda Y, Kimata-Ariga Y, Hase T (2001) Structure of the electron transfer complex between ferredoxin and ferredoxin-NADP(+) reductase. Nat Struct Biol 8: 117-121 doi: 10.1038/84097

Küchler M, Decker S, Hörmann F, Soll J, Heins L (2002) Protein import into chloroplasts involves redox-regulated proteins. EMBO J 21: 6136-6145 doi:

Laisk A, Eichelmann H, Oja V, Talts E, Scheibe R (2007) Rates and roles of cyclic and alternative electron flow in potato leaves. Plant Cell Physiol 48: 1575-1588 doi: 10.1093/pcp/pcm129

Lans I, Medina M, Rosta E, Hummer G, Garcia-Viloca M, Lluch JM, González-Lafont À (2012) Theoretical study of the mechanism of the hydride transfer between ferredoxin-NADP+ reductase and NADP+: the role of Tyr303. J Am Chem Soc 134: 20544-20553 doi: 10.1021/ja310331v

Lans I, Peregrina JR, Medina M, García-Viloca M, González-Lafont A, Lluch JM (2010) Mechanism of the hydride transfer between Anabaena Tyr303Ser FNRrd/FNRox and NADP+/H. A combined pre-steady-state kinetic/ensemble-averaged transition-state theory with multidimensional tunneling study. J Phys Chem B 114: 3368-3379 doi: 10.1021/jp912034m

Lehtimäki N, Koskela MM, Dahlström KM, Pakula E, Lintala M, Scholz M, Hippler M, Hanke GT, Rokka A, Battchikova N, Salminen TA, Mulo P (2014) Posttranslational modifications of FERREDOXIN-NADP+ OXIDOREDUCTASE in Arabidopsis chloroplasts. Plant Physiol 166: 1764-1776 doi: 10.1104/pp.114.249094

Lehtimäki N, Lintala M, Allahverdiyeva Y, Aro EM, Mulo P (2010) Drought stress-induced upregulation of components involved in ferredoxin-dependent cyclic electron transfer. J Plant Physiol 167: 1018-1022 doi: 10.1016/j.jplph.2010.02.006

Lintala M, Allahverdiyeva Y, Kangasjärvi S, Lehtimäki N, Keränen M, Rintamäki E, Aro EM, Mulo P (2009) Comparative analysis of leaf-type ferredoxin-NADP oxidoreductase isoforms in Arabidopsis thaliana. Plant J 57: 1103-1115 doi: 10.1111/j.1365-313X.2008.03753.x

Lintala M, Allahverdiyeva Y, Kidron H, Piippo M, Battchikova N, Suorsa M, Rintamäki E, Salminen TA, Aro EM, Mulo P (2007) Structural and functional characterization of ferredoxin-NADP+-oxidoreductase using knock-out mutants of Arabidopsis. Plant J 49: 1041-1052 doi: 10.1111/j.1365-313X.2006.03014.x

Lintala M, Lehtimäki N, Benz JP, Jungfer A, Soll J, Aro EM, Bölter B, Mulo P (2012) Depletion of leaf-type ferredoxin-NADP(+) oxidoreductase results in the permanent induction of photoprotective mechanisms in Arabidopsis chloroplasts. Plant J 70: 809-817 doi: 10.1111/j.1365-313X.2012.04930.x

Martínez-Júlvez M, Hermoso J, Hurley JK, Mayoral T, Sanz-Aparicio J, Tollin G, Gómez-Moreno C, Medina M (1998a) Role of Arg100 and Arg264 from Anabaena PCC 7119 ferredoxin-NADP+ reductase for optimal NADP+ binding and electron transfer. Biochemistry 37: 17680-17691 doi:

Martínez-Júlvez M, Medina M, Hurley JK, Hafezi R, Brodie TB, Tollin G, Gómez-Moreno C (1998b) Lys75 of Anabaena ferredoxin-NADP+ reductase is a critical residue for binding ferredoxin and flavodoxin during electron transfer. Biochemistry 37: 13604-13613 doi: 10.1021/bi9807411 bi9807411 [pii]
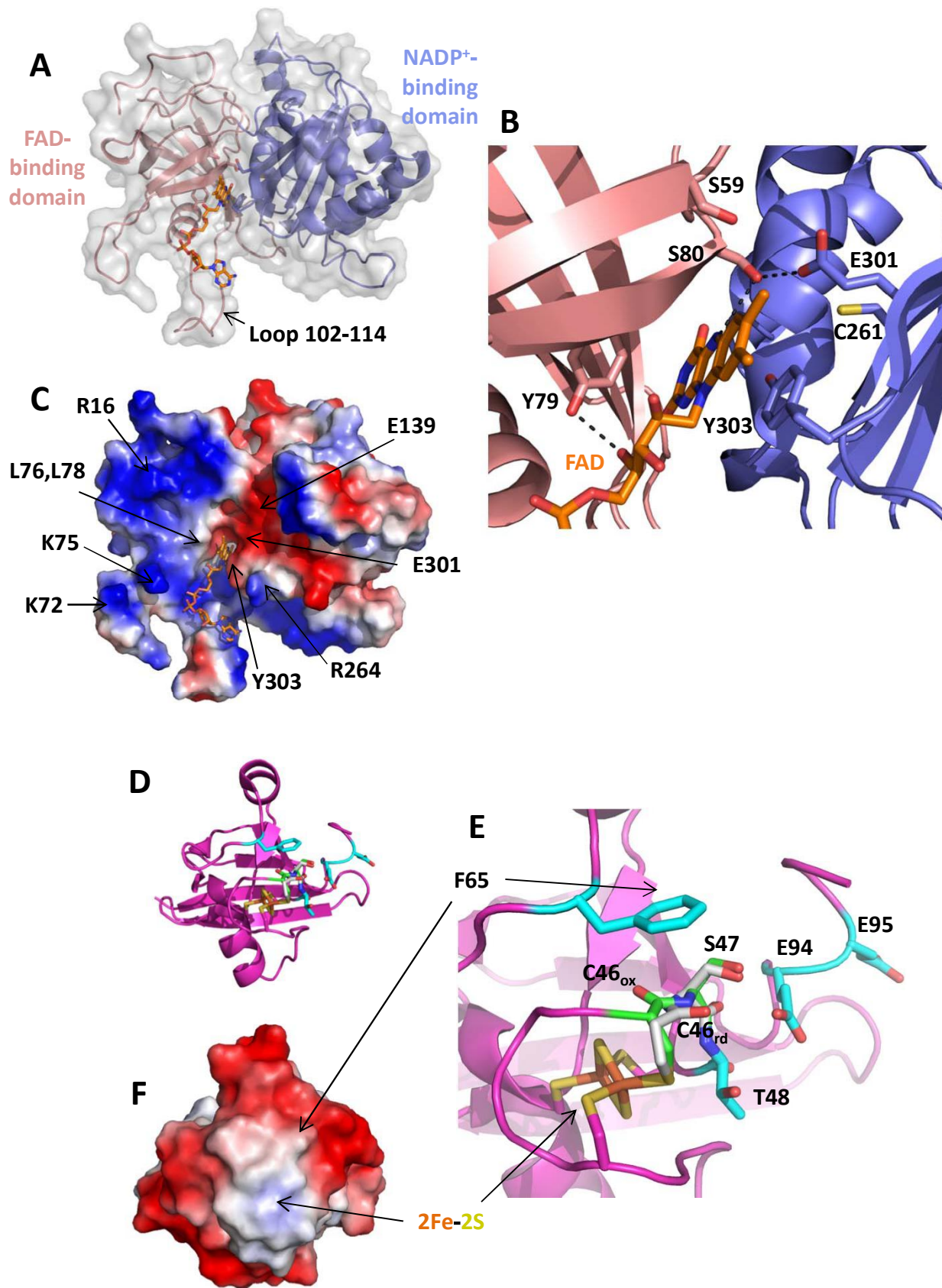
(For nomenclature and classification of FNR isoforms in different higher plant species, please see Mulo 2011)

Martínez-Júlvez M, Medina M, Velázquez-Campoy A (2009) Binding thermodynamics of ferredoxin:NADP+ reductase: two different protein substrates and one energetics. Biophys J 96: 4966-4975 doi: S0006-3495(09)00682-1 [pii] 10.1016/j.bpj.2009.02.061

Martínez-Júlvez M, Nogués I, Faro M, Hurley JK, Brodie TB, Mayoral T, Sanz-Aparicio J, Hermoso JA, Stankovich MT, Medina M, Tollin G, Gómez-Moreno C (2001) Role of a cluster of hydrophobic residues near the FAD cofactor in Anabaena PCC 7119 ferredoxin-NADP+ reductase for optimal complex formation and electron transfer to ferredoxin. J Biol Chem 276: 27498-27510 doi: 10.1074/jbc.M102112200 M102112200 [pii]

Matthijs HC, Coughlan SJ, Hind G (1986) Removal of ferredoxin:NADP+ oxidoreductase from thylakoid membranes, rebinding to depleted membranes, and identification of the binding site. J Biol Chem 261: 12154-12158 doi:

Mayoral T, Martínez-Júlvez M, Pérez-Dorado I, Sanz-Aparicio J, Gómez-Moreno C, Medina M, Hermoso JA (2005) Structural analysis of interactions for complex formation between ferredoxin-NADP+ reductase and its protein partners. Proteins 59: 592-602 doi: 10.1002/prot.20450

Mayoral T, Medina M, Sanz-Aparicio J, Gomez-Moreno C, Hermoso J (2000) Structural basis of the catalytic role of Glu301 in Anabaena PCC 7119 ferredoxin-NADP(+) reductase revealed by x-ray crystallography. Proteins-Structure Function and Genetics 38: 60-69 doi: 10.1002/(SICI)1097-0134(20000101)38:1<60::AID-PROT7>3.0.CO;2-B

Medina M (2009) Structural and mechanistic aspects of flavoproteins: photosynthetic electron transfer from photosystem I to NADP+. FEBS J 276: 3942-3958 doi: EJB7122 [pii] 10.1111/j.1742-4658.2009.07122.x

Medina M, Abagyan R, Gómez-Moreno C, Fernández-Recio J (2008) Docking analysis of transient complexes: interaction of ferredoxin-NADP+ reductase with ferredoxin and flavodoxin. Proteins 72: 848-862 doi: 10.1002/prot.21979

Medina M, Gomez-Moreno C (2004) Interaction of ferredoxin-NADP(+) reductase with its substrates: optimal interaction for efficient electron transfer. Photosynthesis Research 79: 113-131 doi: 10.1023/B:PRES.0000015386.67746.2c

Medina M, Gomez-Moreno C, Tollin G (1992a) Effects of chemical modification of Anabaena flavodoxin and ferredoxin NADP+ reductase on the kinetics of interprotein electron-transfer reactions. European Journal of Biochemistry 210: 577-583 doi: 10.1111/j.1432-1033.1992.tb17457.x

Medina M, Gómez-Moreno C (2004) Interaction of ferredoxin-NADP+ reductase with its substrates: optimal interaction for efficient electron transfer. Photosynth Res 79: 113-131 doi: 10.1023/B:PRES.0000015386.67746.2c

Medina M, Luquita A, Tejero J, Hermoso J, Mayoral T, Sanz-Aparicio J, Grever K, Gómez-Moreno C (2001) Probing the determinants of coenzyme specificity in ferredoxin-NADP+ reductase by site-directed mutagenesis. J Biol Chem 276: 11902-11912 doi: 10.1074/jbc.M009287200 M009287200 [pii]

Medina M, Martínez-Júlvez M, Hurley JK, Tollin G, Gómez-Moreno C (1998) Involvement of glutamic acid 301 in the catalytic mechanism of ferredoxin-NADP+ reductase from Anabaena PCC 7119. Biochemistry 37: 2715-2728 doi: 10.1021/bi971795y bi971795y [pii]

Medina M, Mendez E, Gomez-Moreno C (1992b) Identification of arginyl residues involved in the binding of ferredoxin-NADP+ reductase from Anabaena sp. PCC 7119 to its substrates. Arch Biochem Biophys 299: 281-286 doi:

Medina M, Méndez E, Gómez-Moreno C (1992c) Lysine residues on ferredoxin-NADP+ reductase from Anabaena sp. PCC 7119 involved in substrate binding. FEBS Lett 298: 25-28 doi: 0014-5793(92)80014-8 [pii]

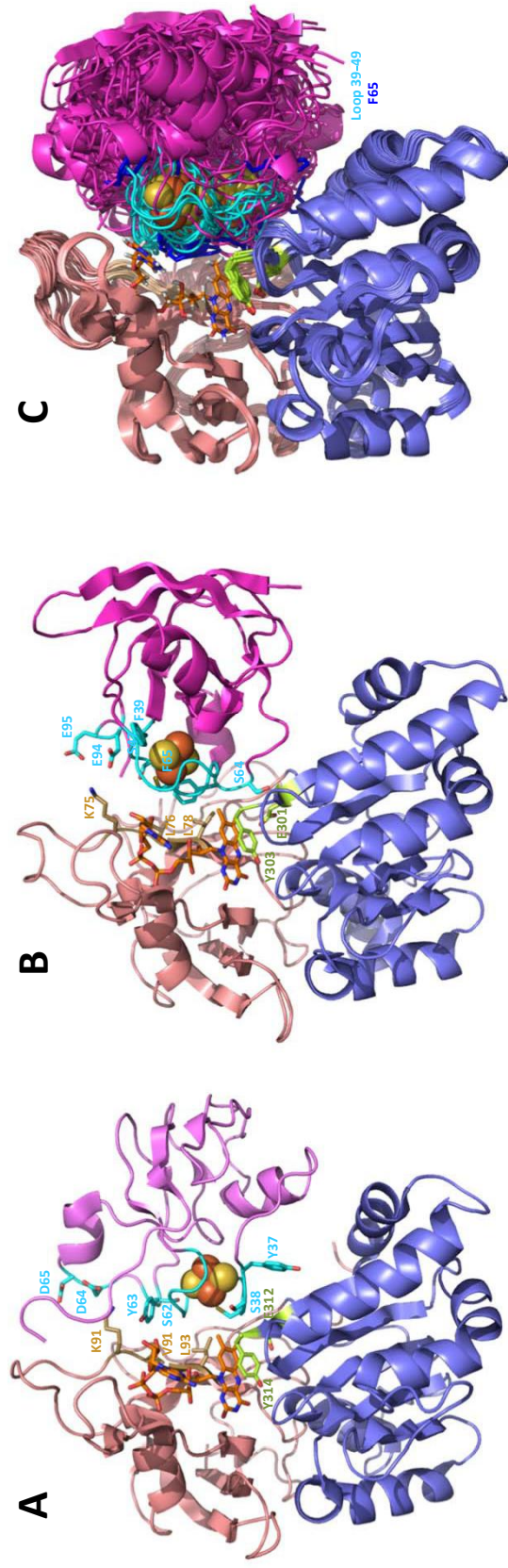(For nomenclature and classification of FNR isoforms in different higher plant species, please see Mulo 2011)

Moolna A, Bowsher CG (2010) The physiological importance of photosynthetic ferredoxin NADP+ oxidoreductase (FNR) isoforms in wheat. J Exp Bot 61: 2669-2681 doi: 10.1093/jxb/erq101

Morales R, Charon MH, Hudry-Clergeon G, Petillot Y, Norager S, Medina M, Frey M (1999) Refined X-ray structures of the oxidized, at 1.3 Å, and reduced, at 1.17 Å, [2Fe-2S] ferredoxin from the cyanobacterium Anabaena PCC7119 show redox-linked conformational changes. Biochemistry 38: 15764-15773 doi: bi991578s [pii]

Morales R, Charon MH, Kachalova G, Serre L, Medina M, Gómez-Moreno C, Frey M (2000) A redox-dependent interaction between two electron-transfer partners involved in photosynthesis. EMBO Rep 1: 271-276 doi: 10.1093/embo-reports/kvd057

Morigasaki S, Jin T, Wada K (1993) Comparative Studies on Ferredoxin-NADP+ Oxidoreductase Isoenzymes Derived from Different Organs by Antibodies Specific for the Radish Root- and Leaf-Enzymes. Plant Physiol 103: 435-440 doi:

Mulo P (2011) Chloroplast-targeted ferredoxin-NADP+ oxidoreductase (FNR): structure, function and location. Biochim Biophys Acta 1807: 927-934 doi: S0005-2728(10)00709-7 [pii] 10.1016/j.bbabio.2010.10.001

Muraki N, Seo D, Shiba T, Sakurai T, Kurisu G (2010) Asymmetric dimeric structure of ferredoxin-NAD(P)+ oxidoreductase from the green sulfur bacterium Chlorobaculum tepidum: implications for binding ferredoxin and NADP+. J Mol Biol 401: 403-414 doi: S0022-2836(10)00640-6 [pii] 10.1016/j.jmb.2010.06.024

Musumeci MA, Arakaki AK, Rial DV, Catalano-Dupuy DL, Ceccarelli EA (2008) Modulation of the enzymatic efficiency of ferredoxin-NADP(H) reductase by the amino acid volume around the catalytic site. FEBS J 275: 1350-1366 doi: EJB6298 [pii] 10.1111/j.1742-4658.2008.06298.x

Nogués I, Tejero J, Hurley JK, Paladini D, Frago S, Tollin G, Mayhew SG, Gómez-Moreno C, Ceccarelli EA, Carrillo N, Medina M (2004) Role of the C-terminal tyrosine of ferredoxin-nicotinamide adenine dinucleotide phosphate reductase in the electron transfer processes with its protein partners ferredoxin and flavodoxin. Biochemistry 43: 6127-6137 doi: 10.1021/bi049858h

Okutani S, Hanke GT, Satomi Y, Takao T, Kurisu G, Suzuki A, Hase T (2005) Three maize leaf ferredoxin:NADPH oxidoreductases vary in subchloroplast location, expression, and interaction with ferredoxin. Plant Physiol 139: 1451-1459 doi: 10.1104/pp.105.070813

Palatnik JF, Tognetti VB, Poli HO, Rodríguez RE, Blanco N, Gattuso M, Hajirezaei MR, Sonnewald U, Valle EM, Carrillo N (2003) Transgenic tobacco plants expressing antisense ferredoxin-NADP(H) reductase transcripts display increased susceptibility to photo-oxidative damage. Plant J 35: 332-341 doi:

Palatnik JF, Valle EM, Carrillo N (1997) Oxidative stress causes ferredoxin-NADP+ reductase solubilization from the thylakoid membranes in methyl viologen-treated plants. Plant Physiol 115: 1721-1727 doi:

Peregrina JR, Herguedas B, Hermoso JA, Martínez-Júlvez M, Medina M (2009) Protein motifs involved in coenzyme interaction and enzymatic efficiency in Anabaena ferredoxin-NADP+ reductase. Biochemistry 48: 3109-3119 doi: 10.1021/bi802077c 10.1021/bi802077c [pii]

Peregrina JR, Lans I, Medina M (2012) The transient catalytically competent coenzyme allocation into the active site of Anabaena ferredoxin NADP+ -reductase. Eur Biophys J 41: 117-128 doi: 10.1007/s00249-011-0704-5

Peregrina JR, Sánchez-Azqueta A, Herguedas B, Martínez-Júlvez M, Medina M (2010) Role of specific residues in coenzyme binding, charge-transfer complex formation, and catalysis in Anabaena ferredoxin-NADP+ reductase. Biochim Biophys Acta 1797: 1638-1646 doi: S0005-2728(10)00580-3 [pii] 10.1016/j.bbabio.2010.05.006

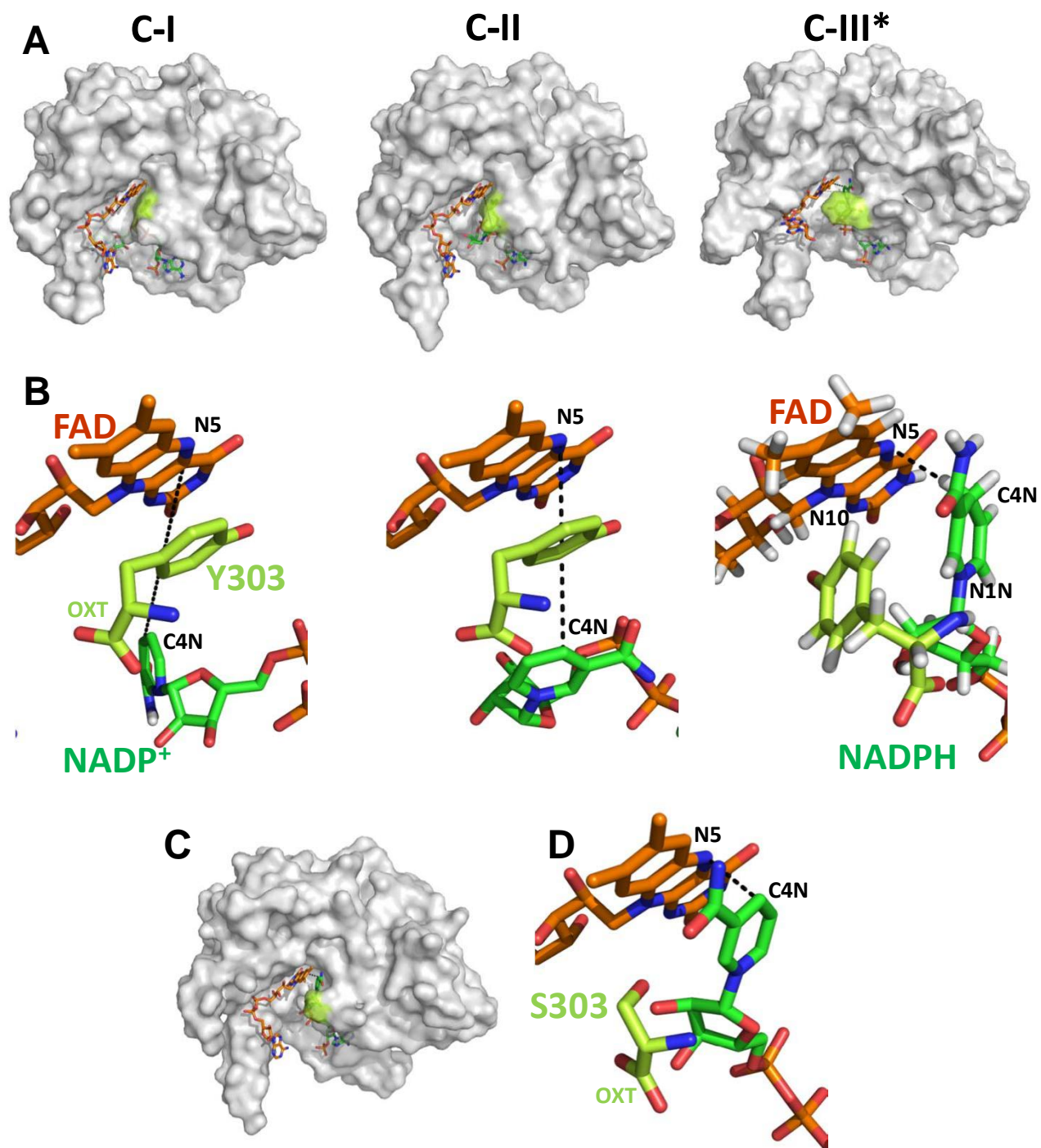(For nomenclature and classification of FNR isoforms in different higher plant species, please see Mulo 2011)

Pessino S, Caelles C, Puigdomènech P, Vallejos RH (1994) Structure and characterization of the gene encoding the ferredoxin-NADP reductase-binding protein from Zea mays L. Gene 147: 205-208 doi:

Piubelli L, Aliverti A, Arakaki AK, Carrillo N, Ceccarelli EA, Karplus PA, Zanetti G (2000) Competition between C-terminal tyrosine and nicotinamide modulates pyridine nucleotide affinity and specificity in plant ferredoxin-NADP+ reductase. J Biol Chem 275: 10472-10476 doi:

Piubelli L, Zanetti G, Bosshard HR (1997) Recombinant wild-type and mutant complexes of ferredoxin and ferredoxin:NADP+ reductase studied by isothermal titration calorimetry. Biol Chem 378: 715-718 doi:

Pueyo JJ, Gómez-Moreno C (1991) Purification of ferredoxin-NADP+ reductase, flavodoxin and ferredoxin from a single batch of the cyanobacterium Anabaena PCC 7119. Prep Biochem 21: 191-204 doi:

Quiles J, Cuello J (1998) Association of ferredoxin-NADP oxidoreductase with the chloroplastic pyridine nucleotide dehydrogenase complex in barley leaves. Plant Physiol 117: 235-244 doi:

Rodriguez RE, Lodeyro A, Poli HO, Zurbriggen M, Peisker M, Palatnik JF, Tognetti VB, Tschiersch H, Hajirezaei MR, Valle EM, Carrillo N (2007) Transgenic tobacco plants overexpressing chloroplastic ferredoxin-NADP(H) reductase display normal rates of photosynthesis and increased tolerance to oxidative stress. Plant Physiol 143: 639-649 doi: 10.1104/pp.106.090449

Rumeau D, Peltier G, Cournac L (2007) Chlororespiration and cyclic electron flow around PSI during photosynthesis and plant stress response. Plant Cell Environ 30: 1041-1051 doi: 10.1111/j.1365-3040.2007.01675.x

Saen-Oon S, Cabeza de Vaca I, Masone D, Medina M, Guallar V (2015) A theoretical multiscale treatment of protein-protein electron transfer: The ferredoxin/ferredoxin-NADP(+) reductase and flavodoxin/ferredoxin-NADP(+) reductase systems. Biochim Biophys Acta 1847: 1530-1538 doi: 10.1016/j.bbabio.2015.09.002

Sancho J, Gómez-Moreno C (1991) Interaction of ferredoxin-NADP+ reductase from Anabaena with its substrates. Arch Biochem Biophys 288: 231-238 doi: 0003-9861(91)90189-P [pii]

Schilder J, Ubbink M (2013) Formation of transient protein complexes. Curr Opin Struct Biol 23: 911-918 doi: 10.1016/j.sbi.2013.07.009

Serre L, Vellieux FM, Medina M, Gómez-Moreno C, Fontecilla-Camps JC, Frey M (1996) X-ray structure of the ferredoxin:NADP+ reductase from the cyanobacterium Anabaena PCC 7119 at 1.8 Å resolution, and crystallographic studies of NADP+ binding at 2.25 Å resolution. J Mol Biol 263: 20-39 doi: S0022-2836(96)90553-7 [pii] 10.1006/jmbi.1996.0553

Setif P (2006) Electron transfer from the bound iron-sulfur clusters to ferredoxin/flavodoxin: kinetic and structural properties of ferredoxin/flavodoxin reduction by photosystem I. In: Golbeck JH (ed) Photosystem I The light-driven platocyanin:ferredoxin oxidoreductase (Advances in Photosynthesis and Respiration.). Springer, Dordrecht, The Netherlands, pp. 439-454.

Shahak Y, Crowther D, Hind G (1981) The involvement of ferredoxin-NADP+ reductase in cyclic electron transport in chloroplasts. Biochim Biophys Acta 636: 234-243 doi:

Shin M, Ishida H, Nozaki Y (1985) A new protein factor, connectein, as a constituent of the large form of ferredoxin NADP+ reductase. Plant Cell Physiol., pp. 559-563.

Shin M, Tsujita M, Tomizawa H, Sakihama N, Kamei K, Oshino R (1990) Proteolytic degradation of ferredoxin-NADP reductase during purification from spinach. Arch Biochem Biophys 279: 97-103 doi:

(For nomenclature and classification of FNR isoforms in different higher plant species, please see Mulo 2011)

Soncini FC, Vallejos RH (1989) The chloroplast reductase-binding protein is identical to the 16.5-kDa polypeptide described as a component of the oxygen-evolving complex. J Biol Chem 264: 21112-21115 doi:

Stengel A, Benz P, Balsera M, Soll J, Bölter B (2008) TIC62 redox-regulated translocon composition and dynamics. J Biol Chem 283: 6656-6667 doi: 10.1074/jbc.M706719200

Suorsa M (2015) Cyclic electron flow provides acclimatory plasticity for the photosynthetic machinery under various environmental conditions and developmental stages. Front Plant Sci 6: 800 doi: 10.3389/fpls.2015.00800

Sánchez-Azqueta A, Catalano-Dupuy DL, López-Rivero A, Tondo ML, Orellano EG, Ceccarelli EA, Medina M (2014a) Dynamics of the active site architecture in plant-type Ferredoxin-NADP(+) reductases catalytic complexes. Biochim Biophys Acta 10.1016/j.bbabio.2014.06.003

Sánchez-Azqueta A, Herguedas B, Hurtado-Guerrero R, Hervás M, Navarro JA, Martínez-Júlvez M, Medina M (2014b) A hydrogen bond network in the active site of Anabaena ferredoxin-NADP(+) reductase modulates its catalytic efficiency. Biochim Biophys Acta 1837: 251-263 doi: 10.1016/j.bbabio.2013.10.010

Sánchez-Azqueta A, Martínez-Júlvez M, Hervás M, Navarro JA, Medina M (2014c) External loops at the ferredoxin-NADP(+) reductase protein-partner binding cavity contribute to substrates allocation. Biochim Biophys Acta 1837: 296-305 doi: 10.1016/j.bbabio.2013.11.016

Sánchez-Azqueta A, Musumeci MA, Martínez-Júlvez M, Ceccarelli EA, Medina M (2012) Structural backgrounds for the formation of a catalytically competent complex with NADP(H) during hydride transfer in ferredoxin-NADP+ reductases. Biochim Biophys Acta 1817: 1063-1071 doi: S0005-2728(12)00131-4 [pii] 10.1016/j.bbabio.2012.04.009

Tejero J, Martínez-Júlvez M, Mayoral T, Luquita A, Sanz-Aparicio J, Hermoso JA, Hurley JK, Tollin G, Gómez-Moreno C, Medina M (2003) Involvement of the pyrophosphate and the 2'-phosphate binding regions of ferredoxin-NADP+ reductase in coenzyme specificity. J Biol Chem 278: 49203-49214 doi: 10.1074/jbc.M307934200 M307934200 [pii]

Tejero J, Peregrina JR, Martínez-Júlvez M, Gutiérrez A, Gómez-Moreno C, Scrutton NS, Medina M (2007) Catalytic mechanism of hydride transfer between NADP+/H and ferredoxin-NADP+ reductase from Anabaena PCC 7119. Arch Biochem Biophys 459: 79-90 doi: S0003-9861(06)00409-7 [pii] 10.1016/j.abb.2006.10.023

Tejero J, Pérez-Dorado I, Maya C, Martínez-Júlvez M, Sanz-Aparicio J, Gómez-Moreno C, Hermoso JA, Medina M (2005) C-terminal tyrosine of ferredoxin-NADP+ reductase in hydride transfer processes with NAD(P)+/H. Biochemistry 44: 13477-13490 doi: 10.1021/bi051278c

Thomas JC, Ughy B, Lagoutte B, Ajlani G (2006) A second isoform of the ferredoxin:NADP oxidoreductase generated by an in-frame initiation of translation. Proc Natl Acad Sci U S A 103: 18368-18373 doi: 10.1073/pnas.0607718103

Twachtmann M, Altmann B, Muraki N, Voss I, Okutani S, Kurisu G, Hase T, Hanke GT (2012) N-terminal structure of maize ferredoxin:NADP+ reductase determines recruitment into different thylakoid membrane complexes. Plant Cell 24: 2979-2991 doi: tpc.111.094532 [pii] 10.1105/tpc.111.094532

Ubbink M (2012) Dynamics in transient complexes of redox proteins. Biochem Soc Trans 40: 415-418 doi: 10.1042/BST20110698

Vallejos RH, Ceccarelli E, Chan R (1984) Evidence for the existence of a thylakoid intrinsic protein that binds ferredoxin-NADP+ oxidoreductase. J Biol Chem 259: 8048-8051 doi:

Velázquez-Campoy A, Goñi G, Peregrina JR, Medina M (2006) Exact analysis of heterotropic interactions in proteins: Characterization of cooperative ligand binding by isothermal

(For nomenclature and classification of FNR isoforms in different higher plant species, please see Mulo 2011)

titration calorimetry. Biophys J 91: 1887-1904 doi: S0006-3495(06)71899-9 [pii] 10.1529/biophysj.106.086561

Vishniac W, Ochoa S (1952) Fixation of carbon dioxide coupled to photochemical reduction of pyridine nucleotides by chloroplast preparations. J Biol Chem 195: 75-93 doi:

Walker MC, Pueyo JJ, Gómez-Moreno C, Tollin G (1990) Comparison of the kinetics of reduction and intramolecular electron transfer in electrostatic and covalent complexes of ferredoxin-NADP+ reductase and flavodoxin from Anabaena PCC 7119. Arch Biochem Biophys 281: 76-83 doi:

Yang C, Hu H, Ren H, Kong Y, Lin H, Guo J, Wang L, He Y, Ding X, Grabsztunowicz M, Mulo P, Chen T, Liu Y, Wu Z, Wu Y, Mao C, Wu P, Mo X (2016) Light-induced rice1 regulates light-dependent attachment of leaf-type ferredoxin-NADP+ oxidoreductase to the thylakoid membrane in rice and Arabidopsis. Plant Cell 28: 712-728 doi: 10.1105/tpc.15.01027

Zanetti G, Aliverti A, Curti B (1984) A cross-linked complex between ferredoxin and ferredoxin-NADP+ reductase. J Biol Chem 259: 6153-6157 doi:

Zanetti G, Gozzer C, Sacchi G, Curti B (1979) Modification of arginyl residues in ferredoxin-NADP+ reductase from spinach leaves. Biochim Biophys Acta 568: 127-134 doi:

Zhang H, Whitelegge JP, Cramer WA (2001) Ferredoxin:NADP+ oxidoreductase is a subunit of the chloroplast cytochrome b6f complex. J Biol Chem 276: 38159-38165 doi: 10.1074/jbc.M105454200 M105454200 [pii]

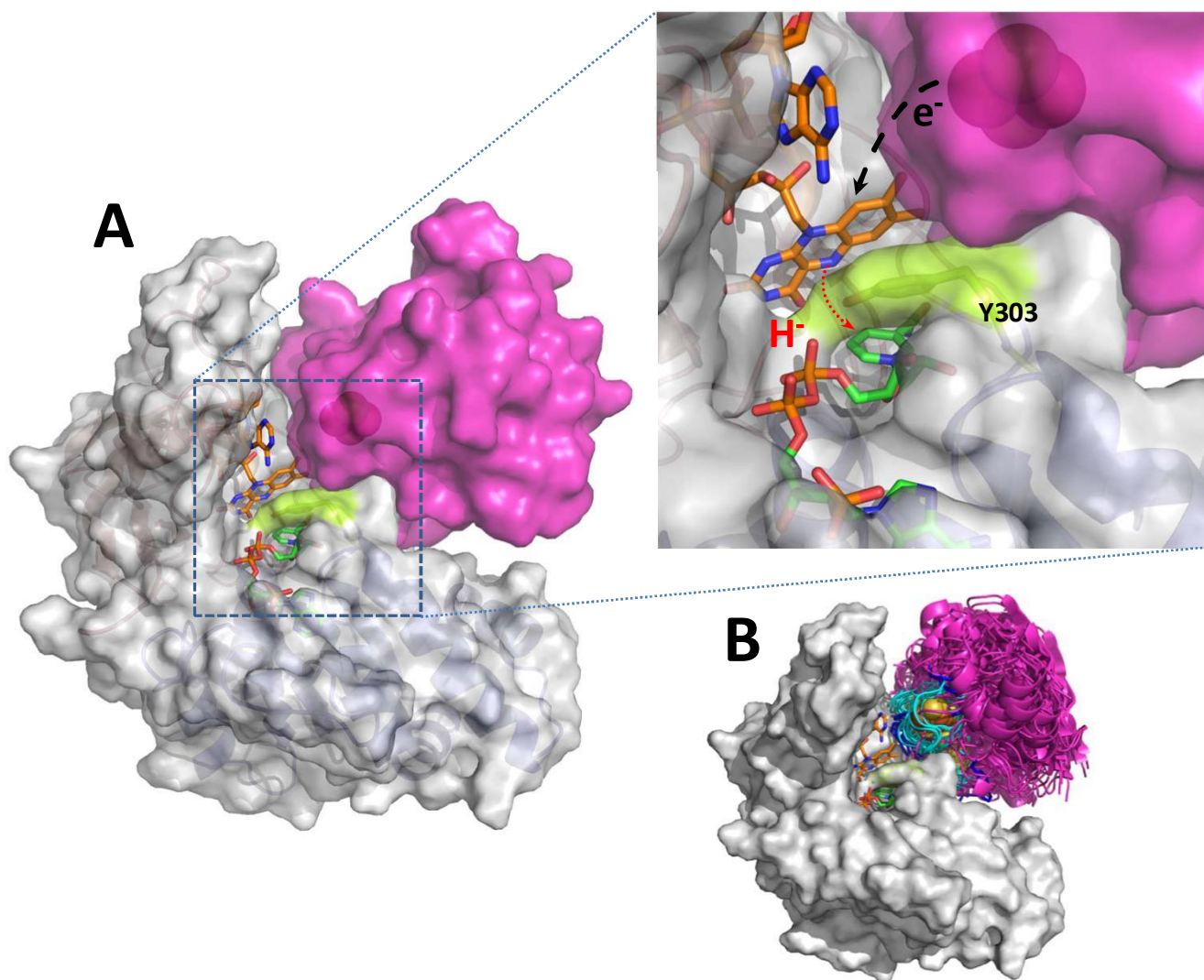(For nomenclature and classification of FNR isoforms in different higher plant species, please see Mulo 2011)

Figure 1

Figure 2

Figure 3

A   C-I   C-II   C-III*

B   FAD   N5   N5   FAD   N5
     Y303   N10   C4N
     OXT   C4N   C4N   N1N
     NADP⁺   NADPH

C   D   N5   C4N
          S303
          OXT

Figure 4

Figure 5